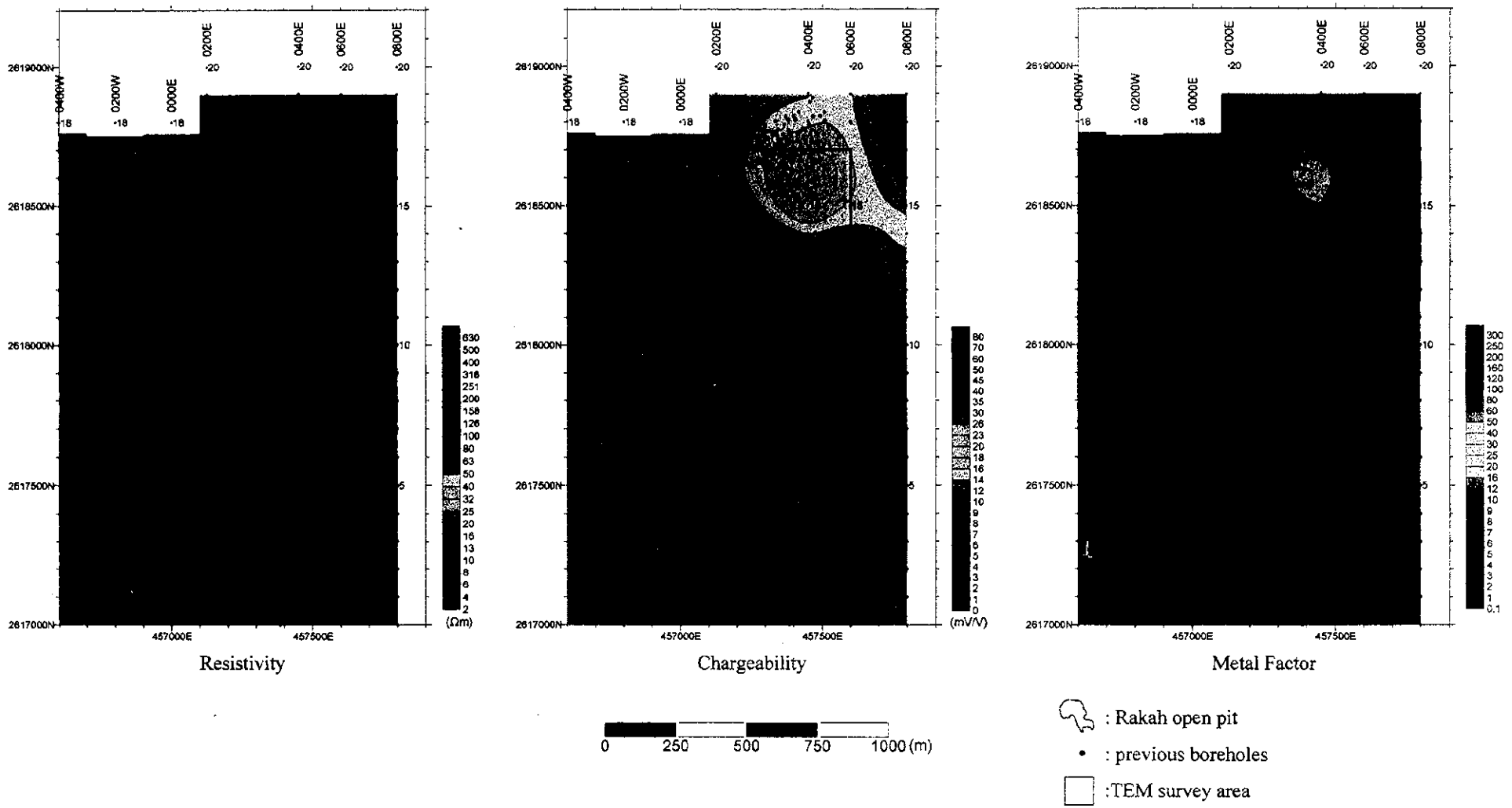

Fig. II-5-18(3) 2D analysis plane maps in Rakah Mine area at 200m depth

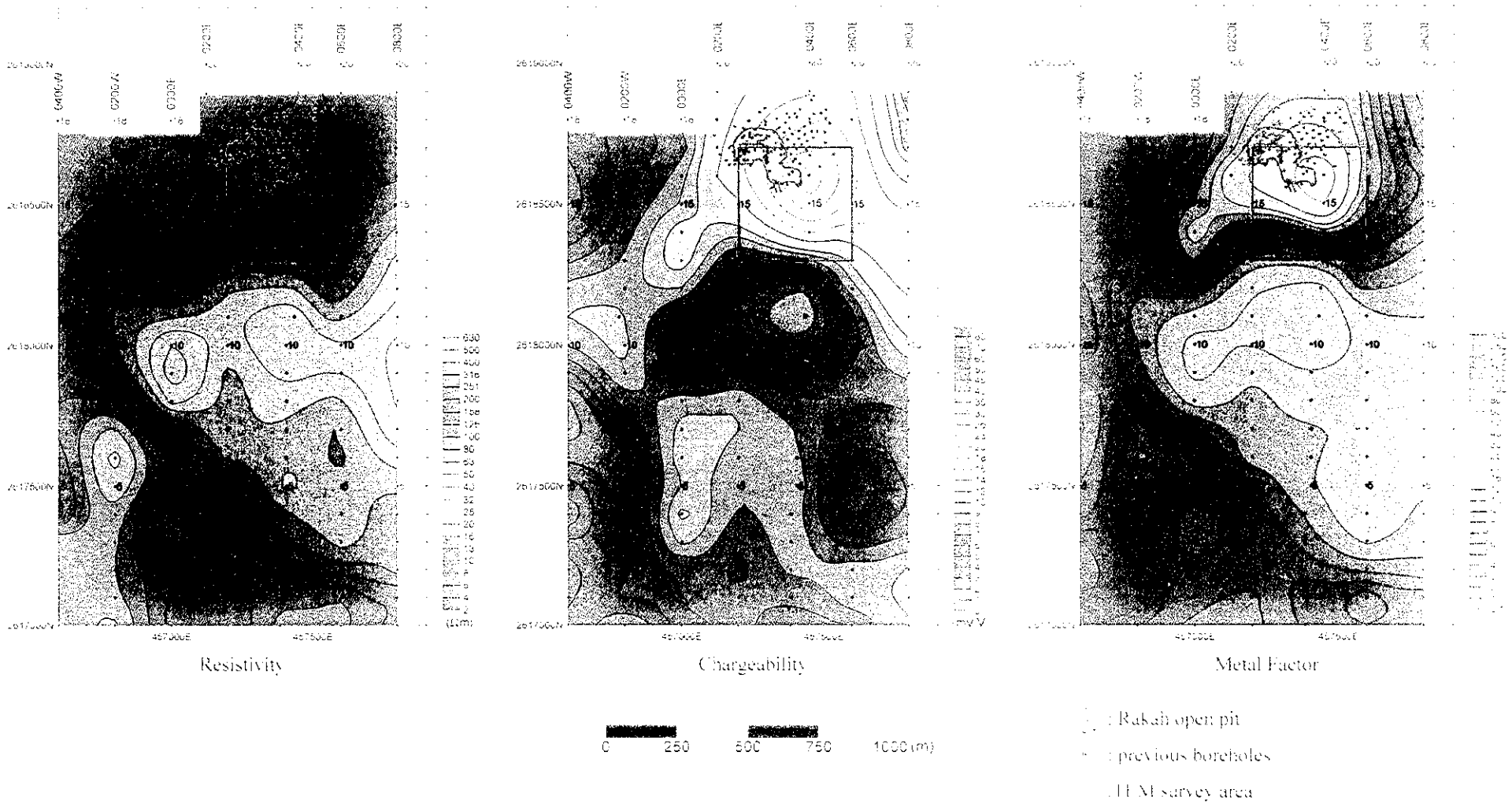

Fig. II-5-18(3) 2D analysis plane maps in Rakah Mine area at 200m depth

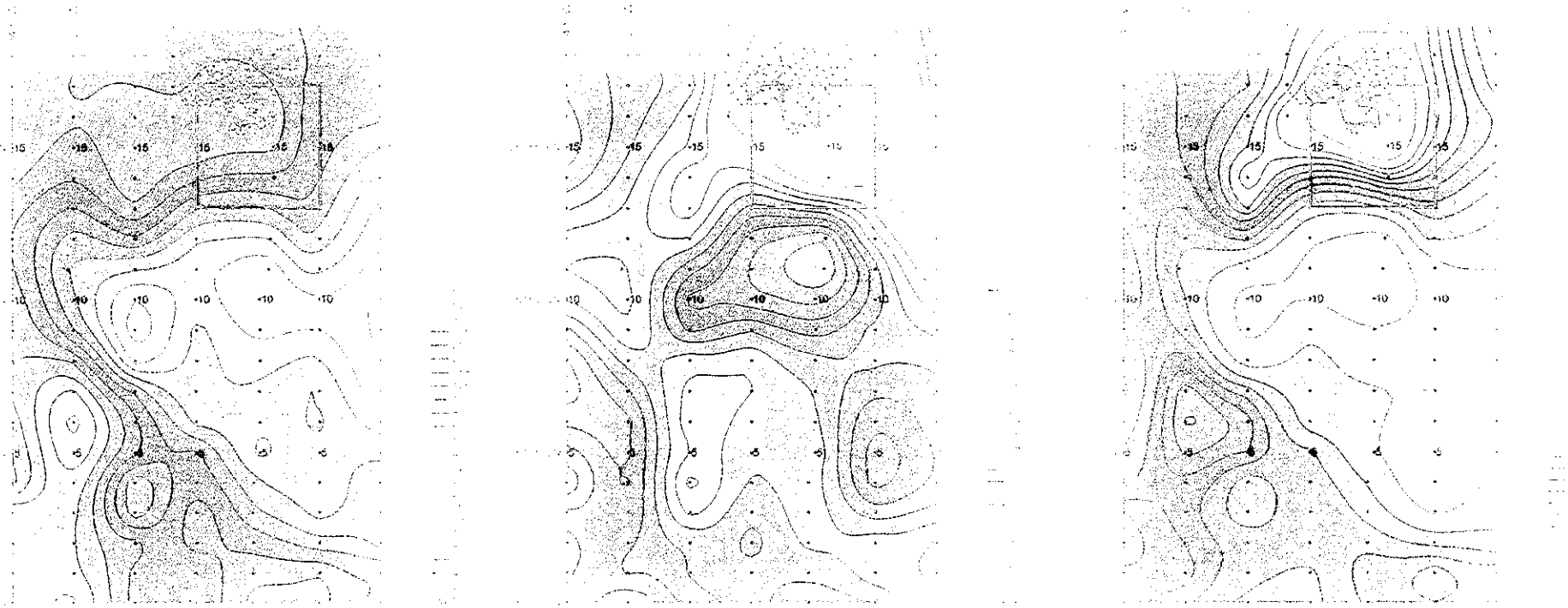
-15
-10
-5

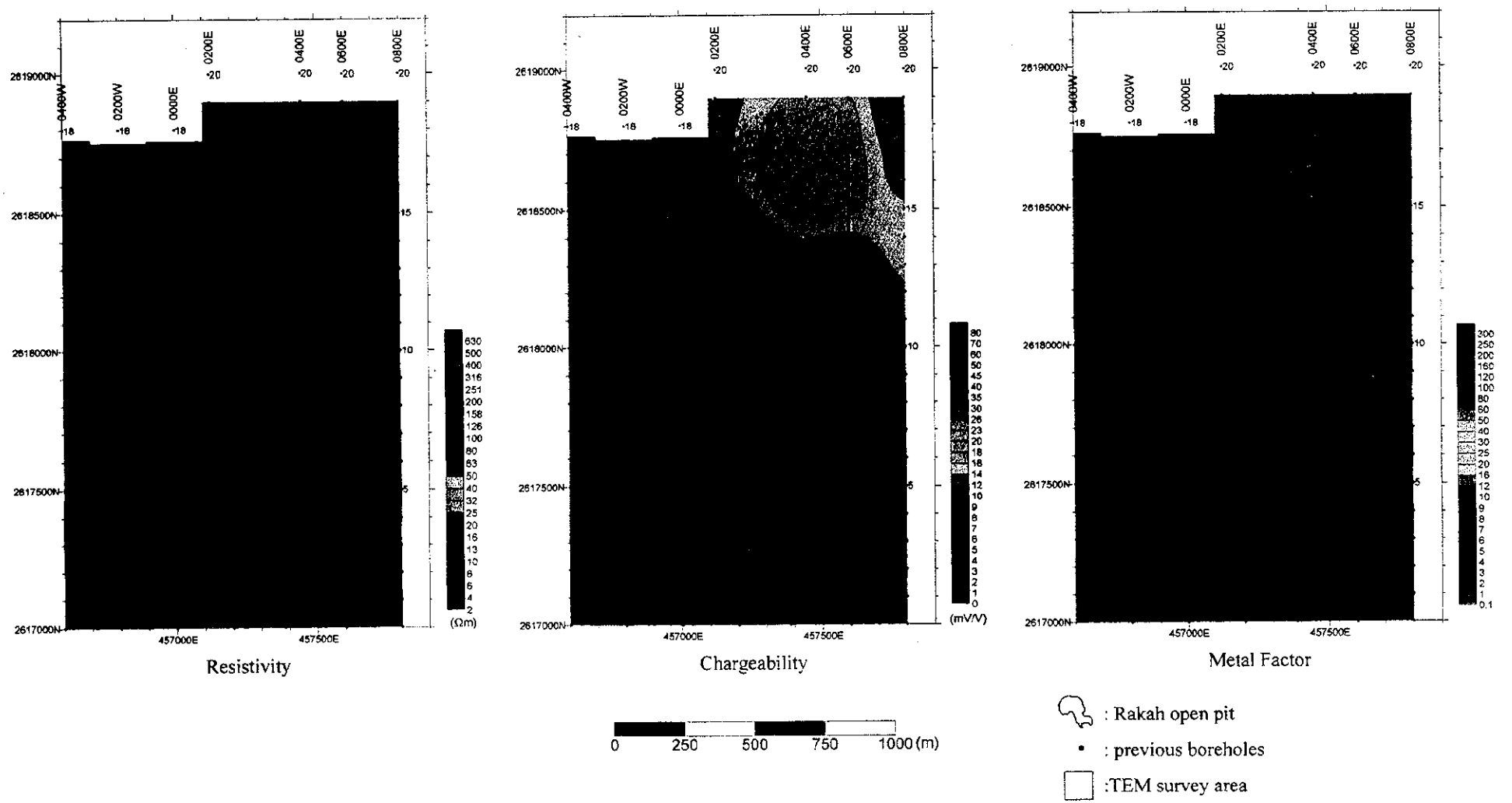

Fig. Ⅱ-5-18(4) 2D analysis plane maps in Rakah Mine area at 250m depth

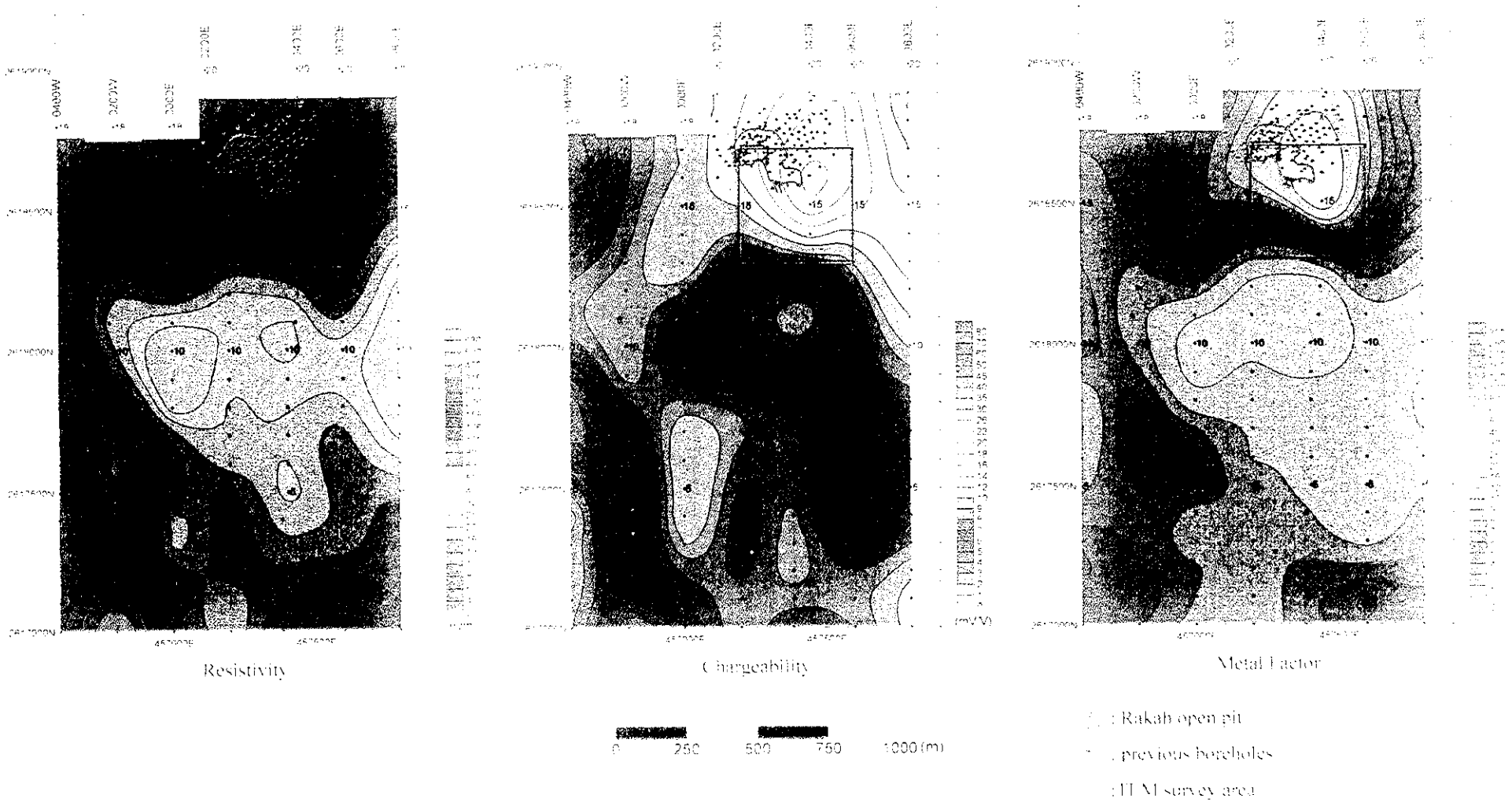

Fig. II-5-18(4) 2D analysis plane maps in Rakah Mine area at 250m depth

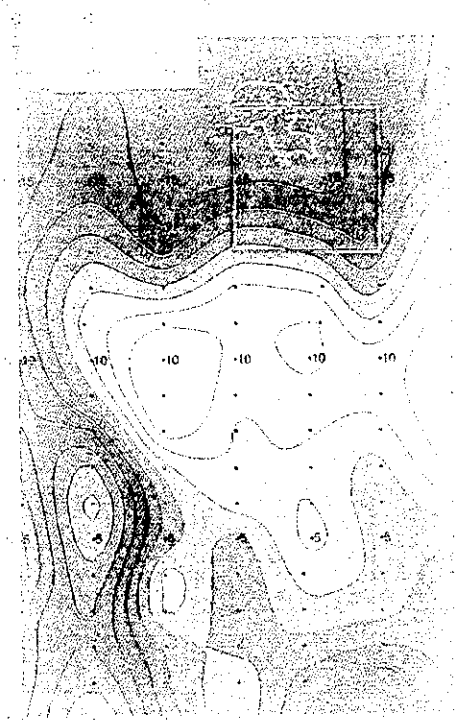

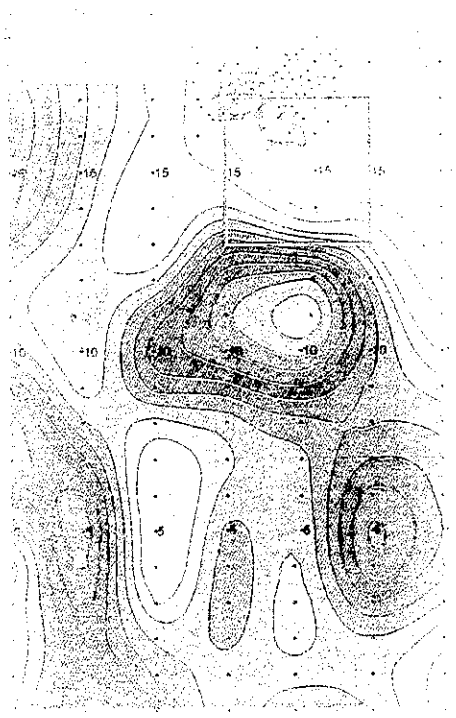

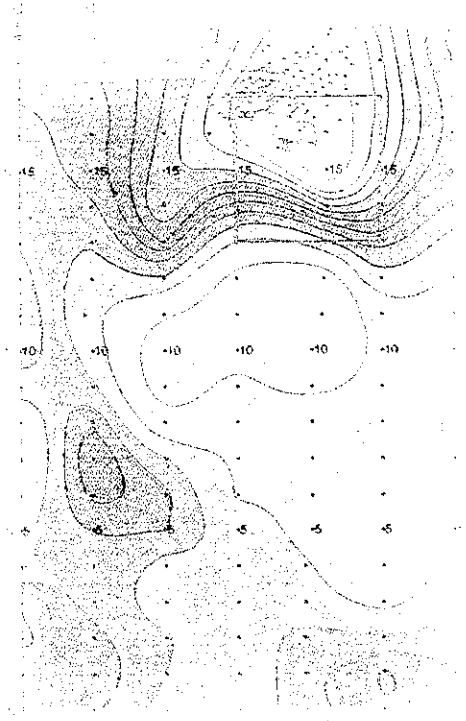

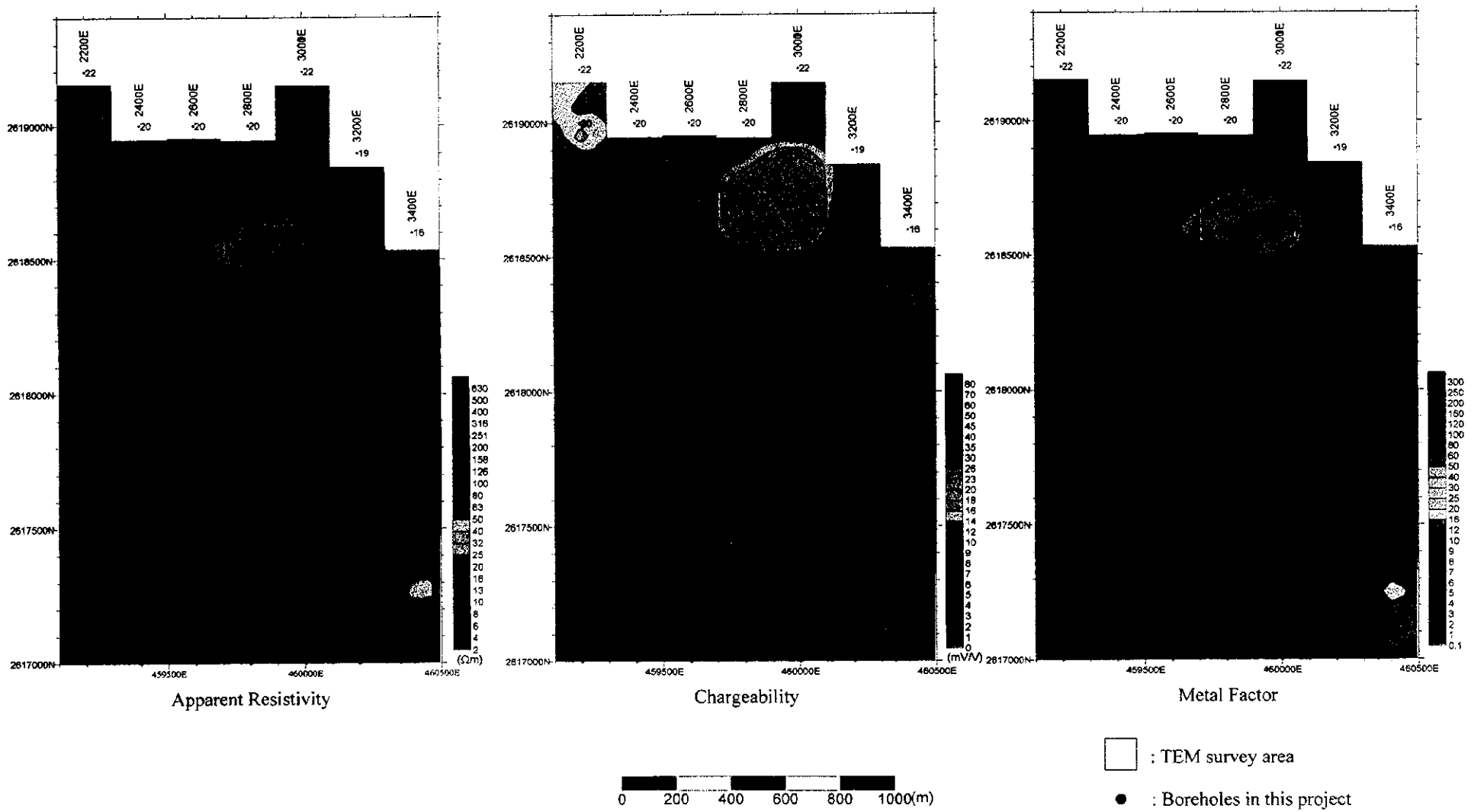

Fig. II-5-19(1) TDIP plane maps in Quron Al-Akhbab area for N=1

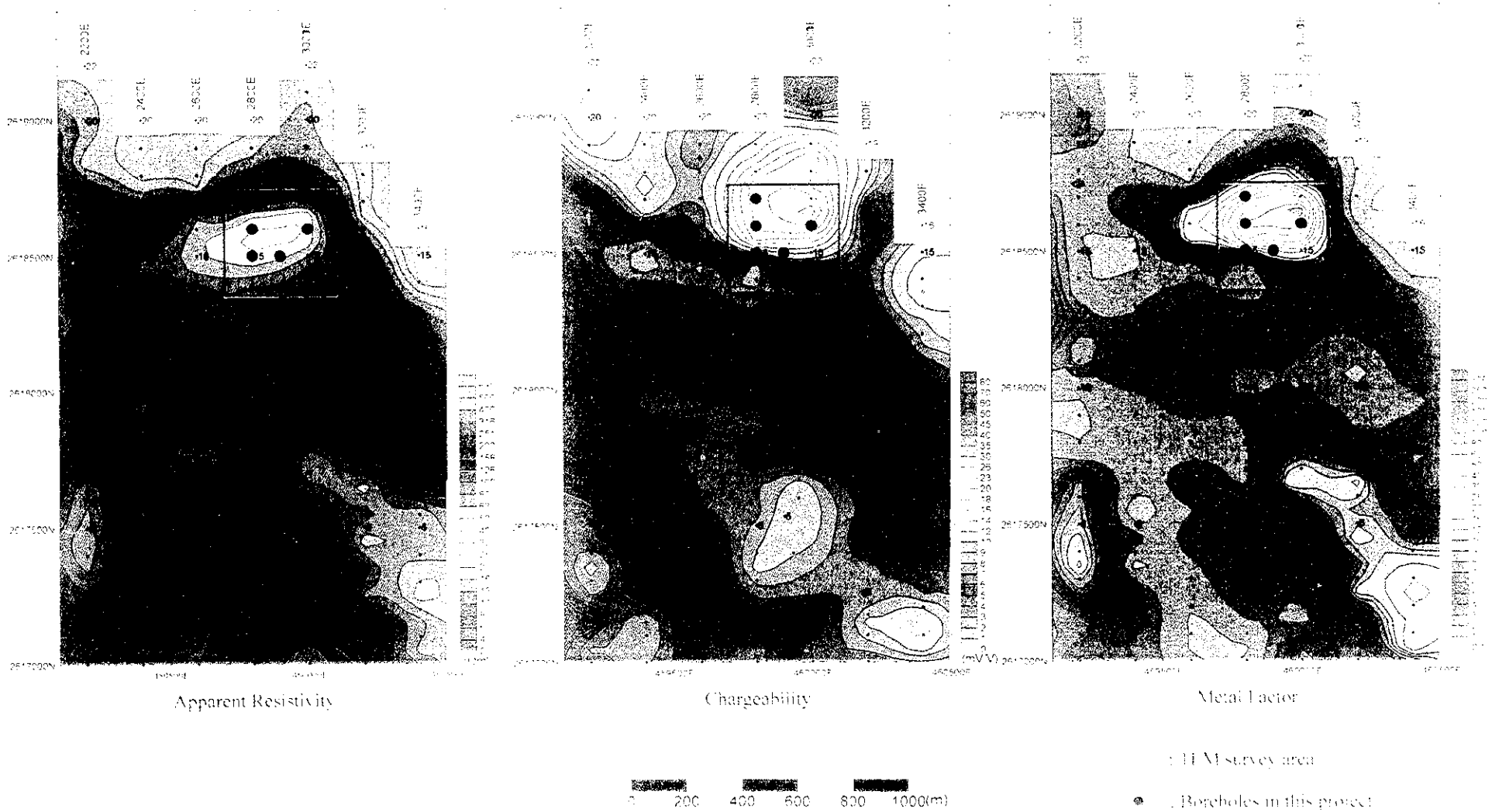

Fig. II-5-1-9(1) IDIP plane maps in Quron Al-Akhbab area for N=1

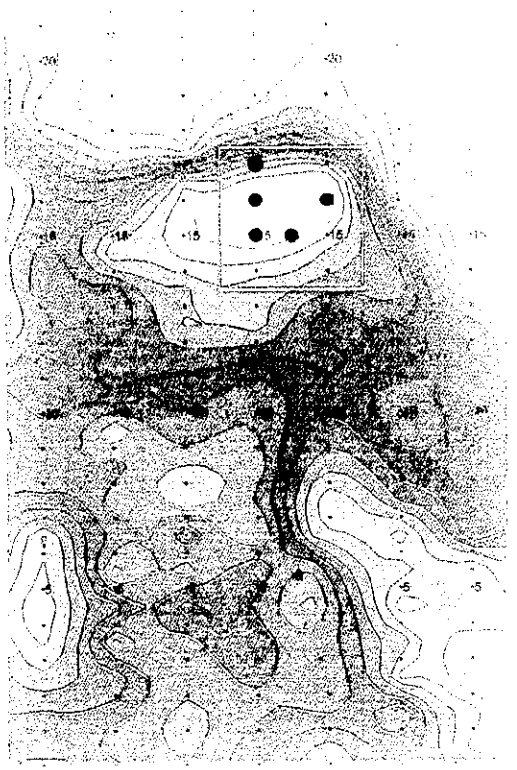

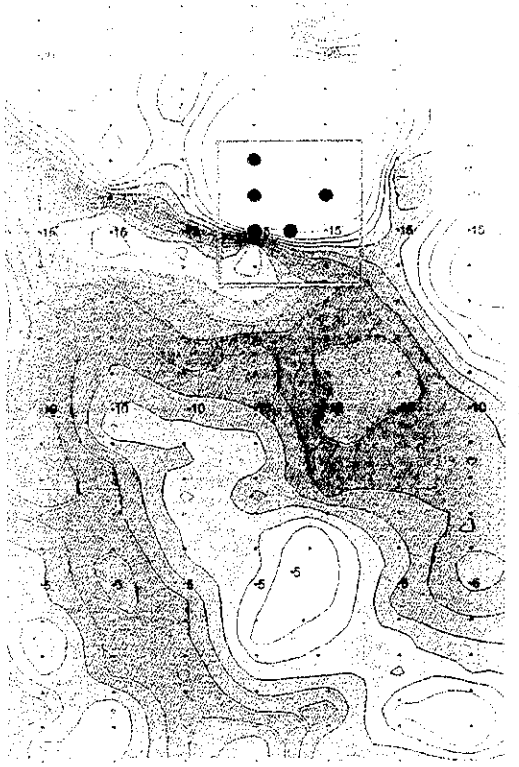

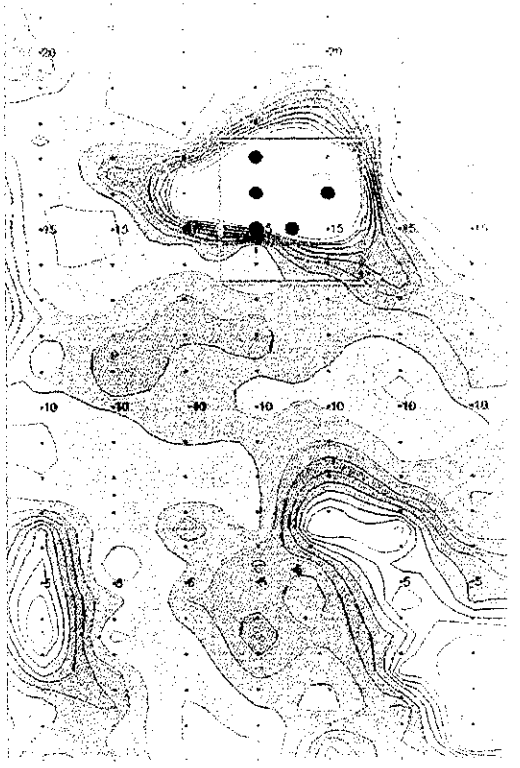

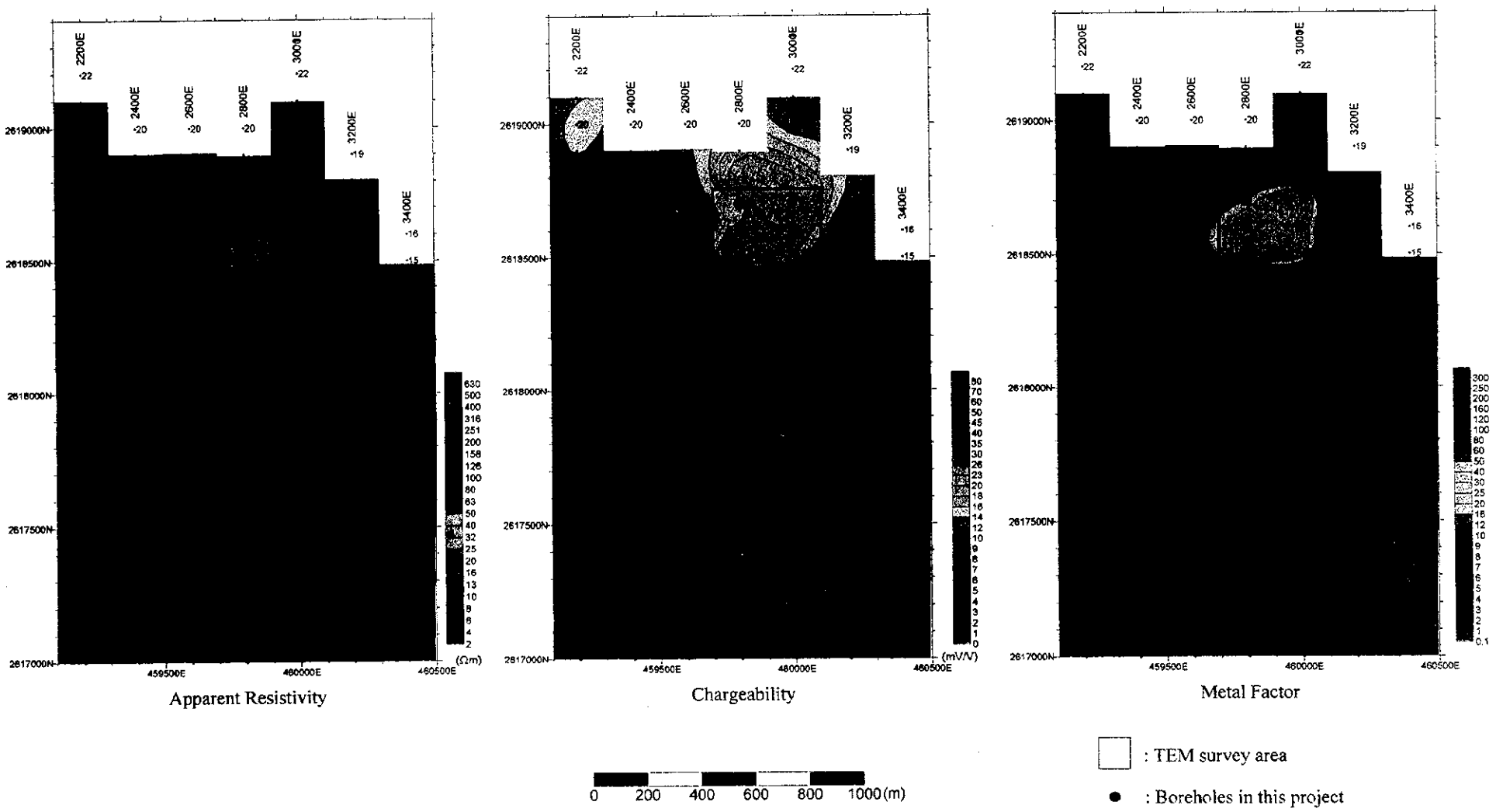

Fig. II -5-19(2) TDIP plane maps in Quron Al-Akhbab area for N=2

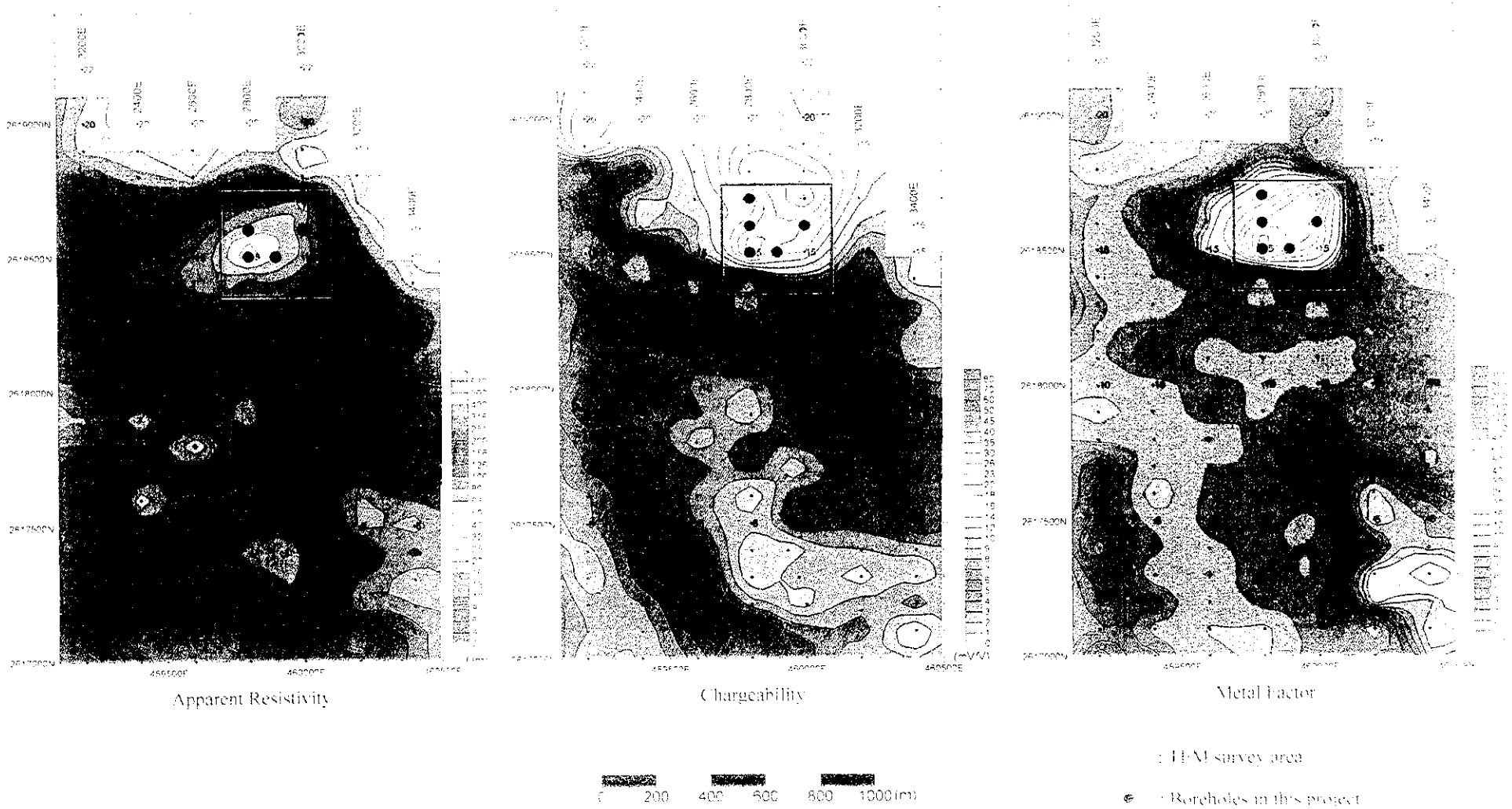

Fig. II-5-19(2) IDIP plane maps in Quron Al-Akhbab area for N-2

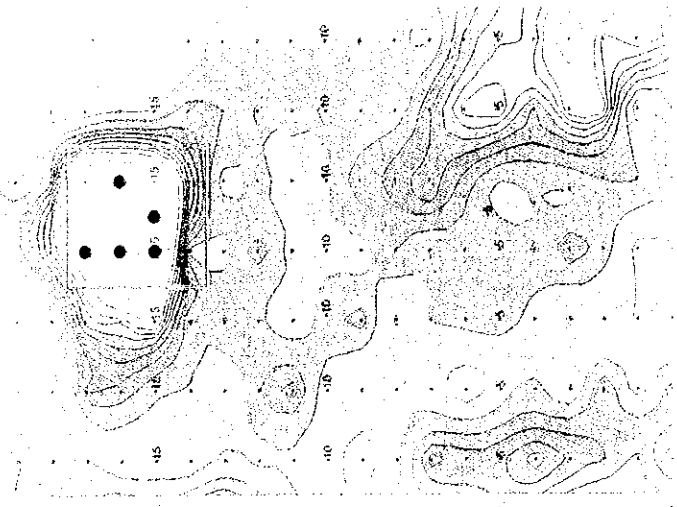

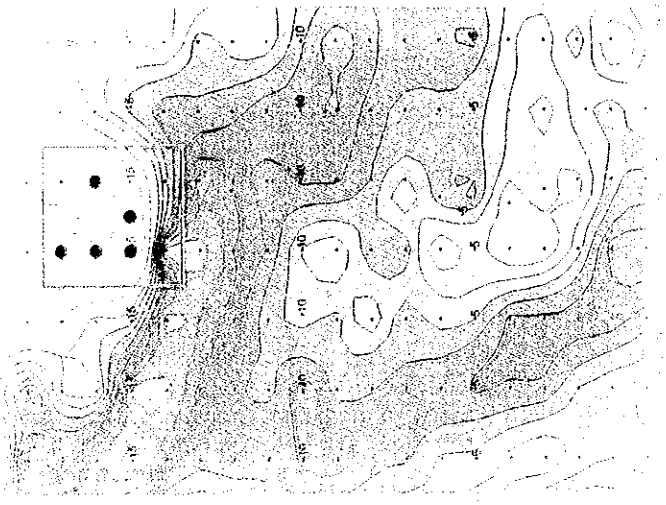

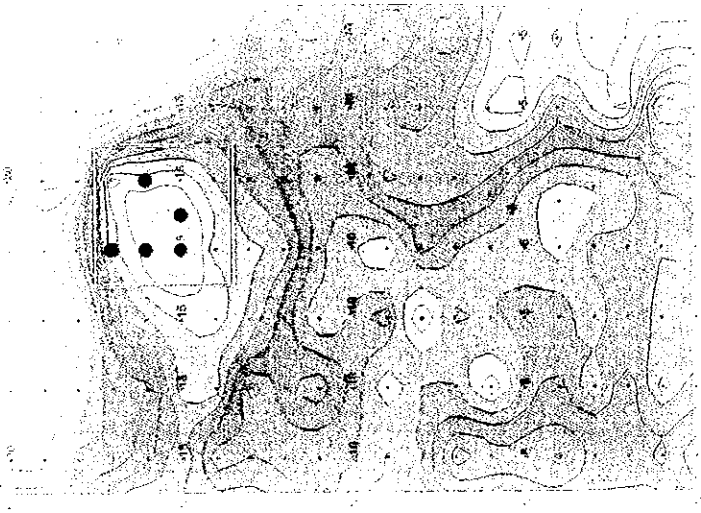

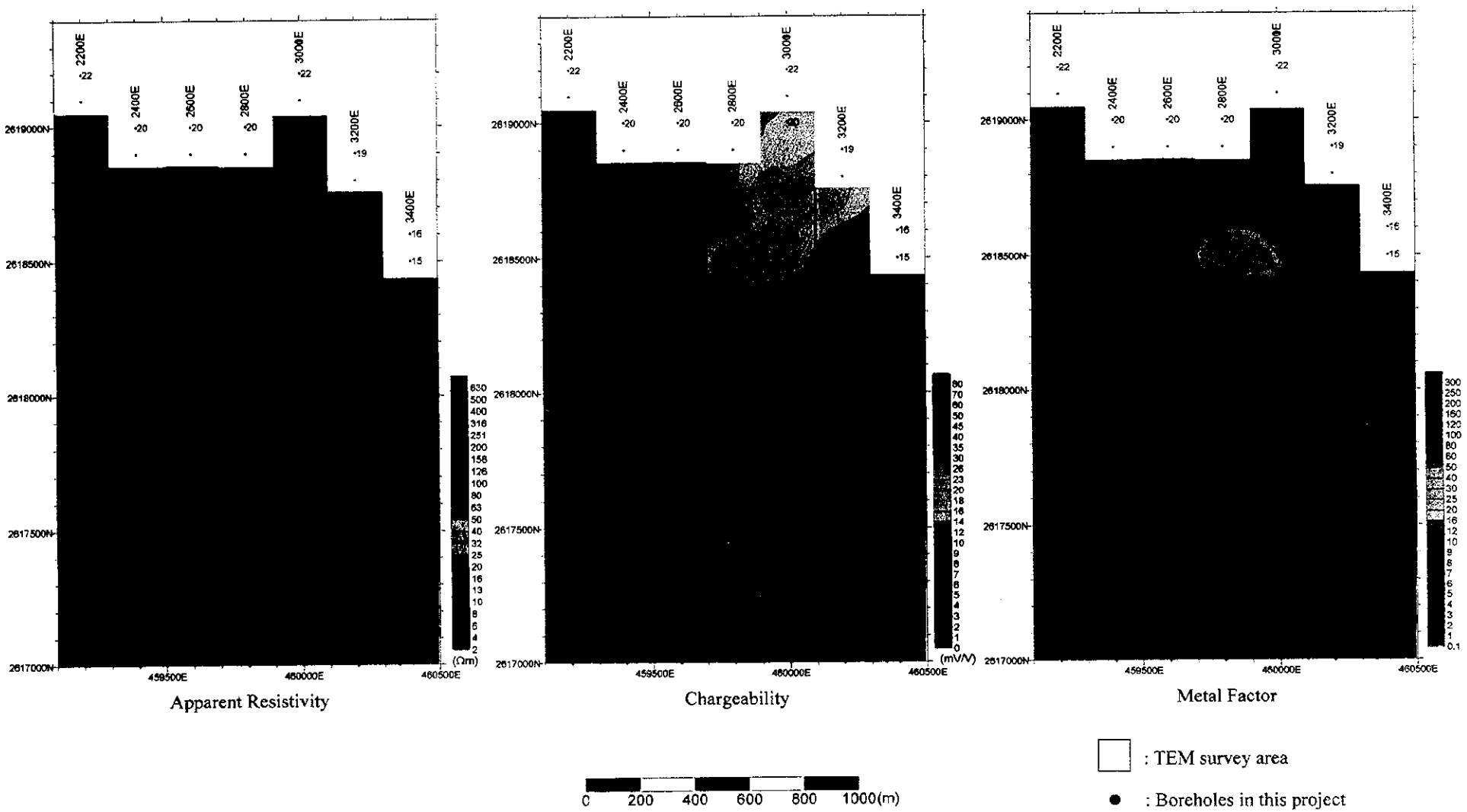

Fig. II -5-19(3) TDIP plane maps in Quron Al-Akhbab area for N=3

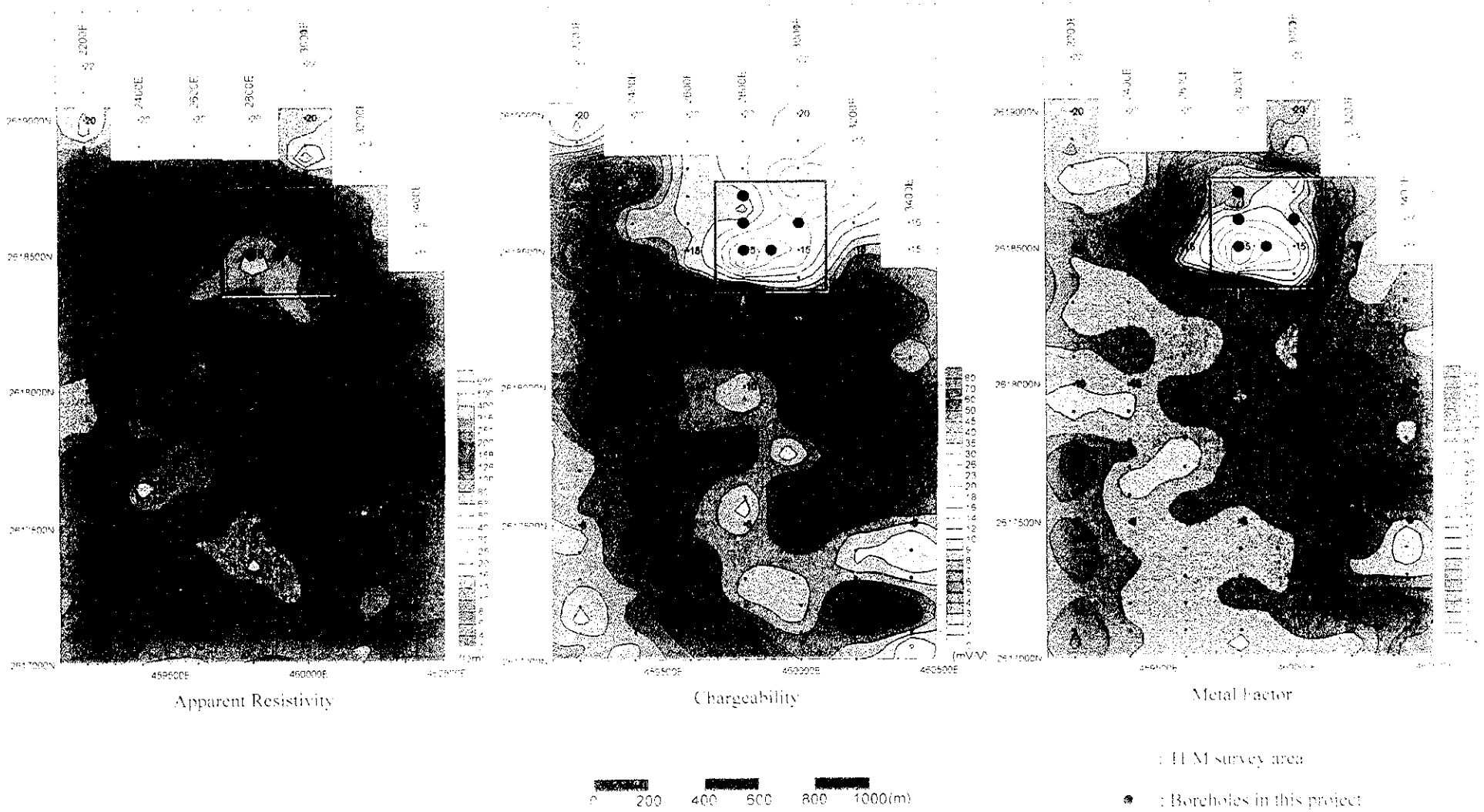

Fig. B-5-19(3) IDIP plane maps in Quron Al-Akhbab area for N-3

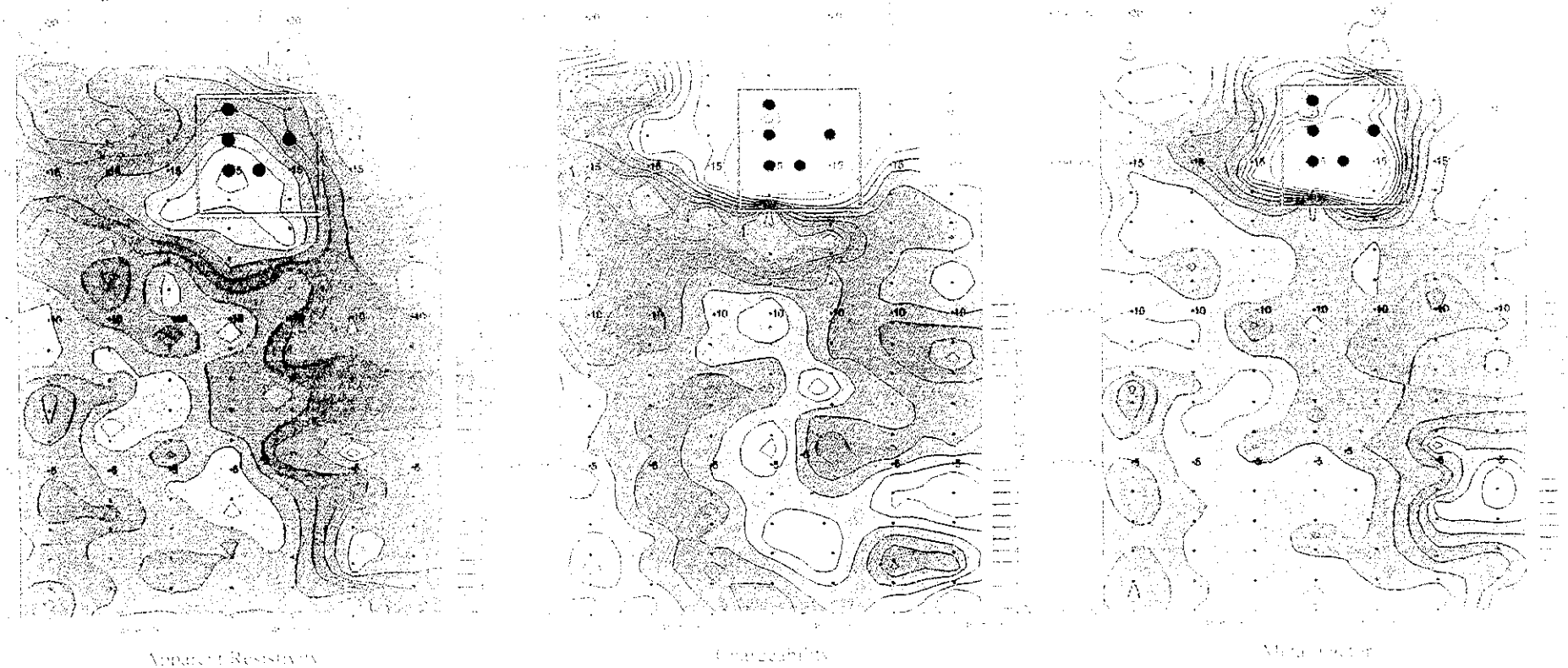

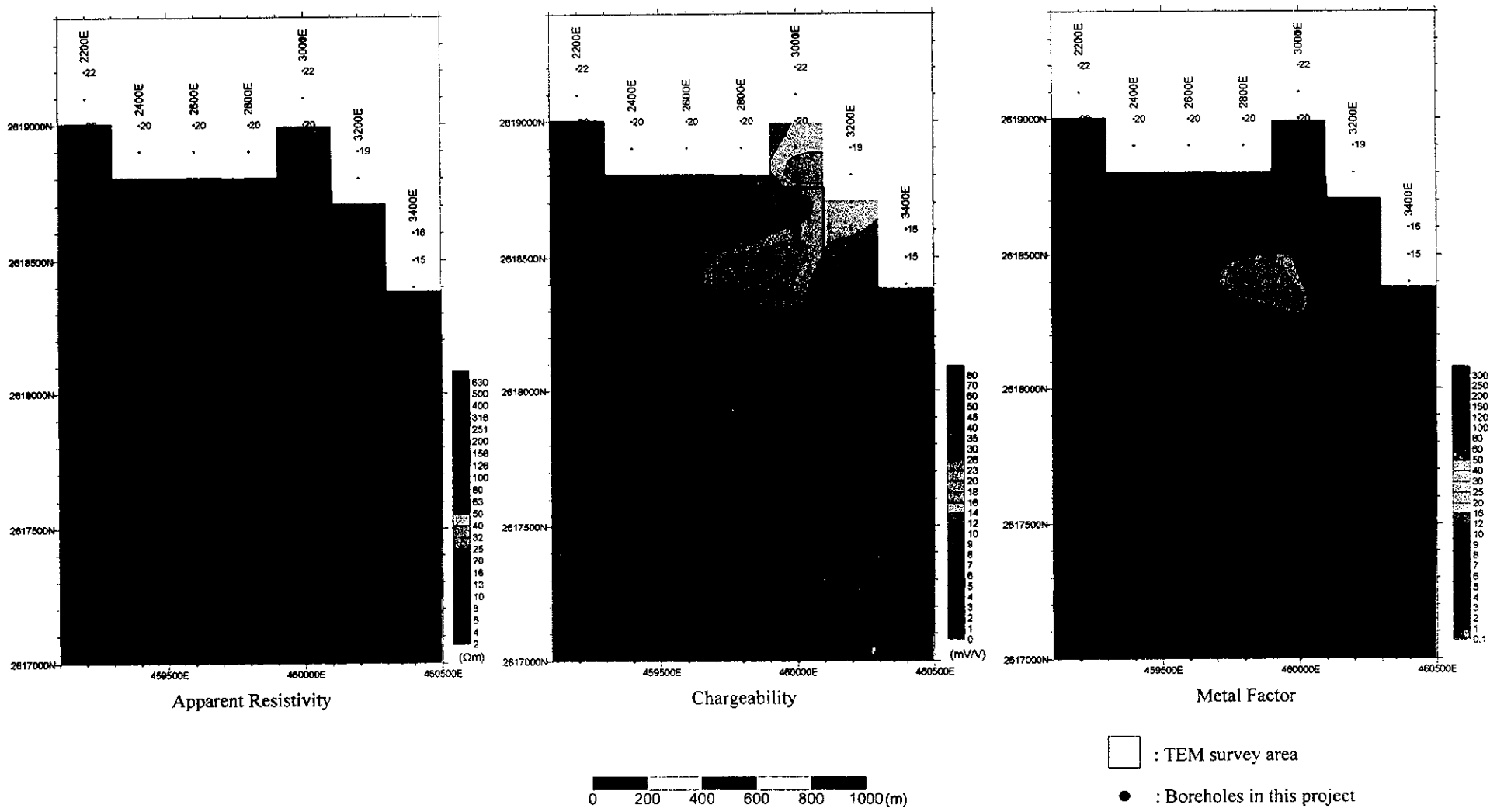

Fig. II -5-19(4) TDIP plane maps in Quron Al-Akhbab area for N=4

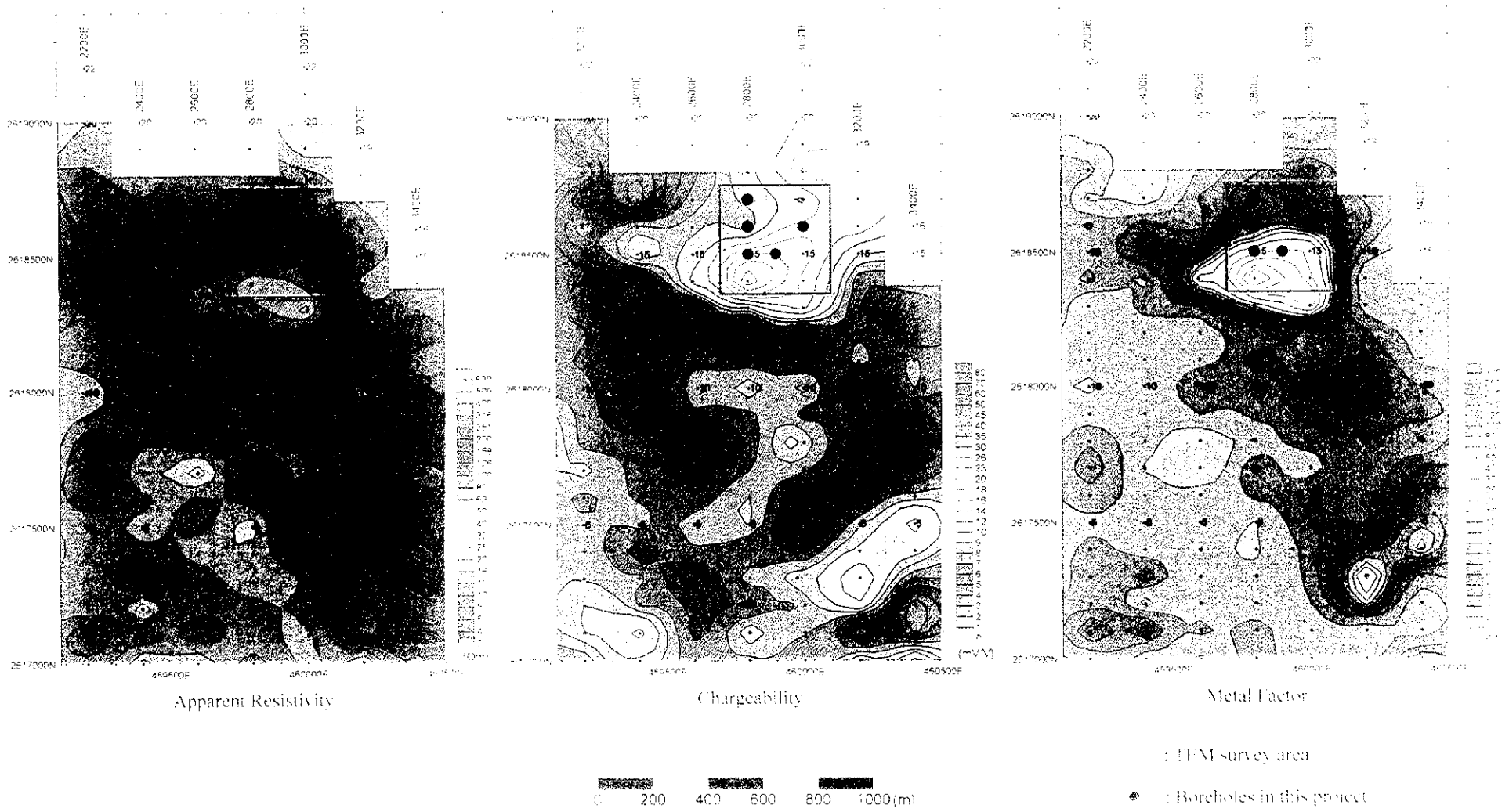

Fig. II-5-19(4) IDIP plane maps in Quron Al-Akhbab area for N-4

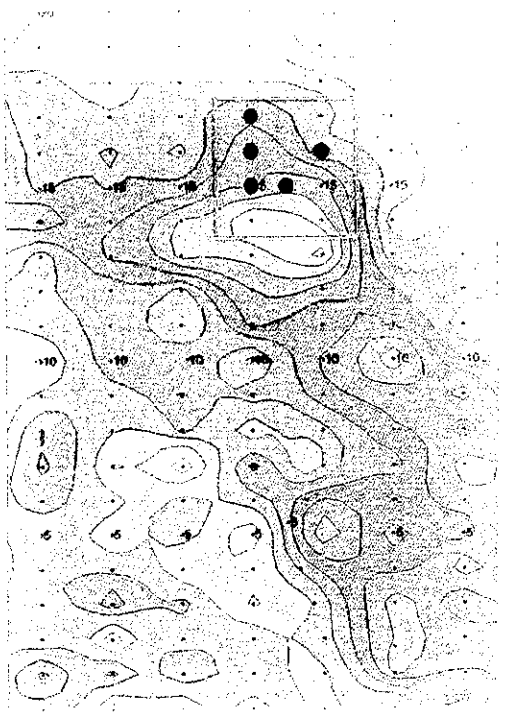
-15
-10
-5

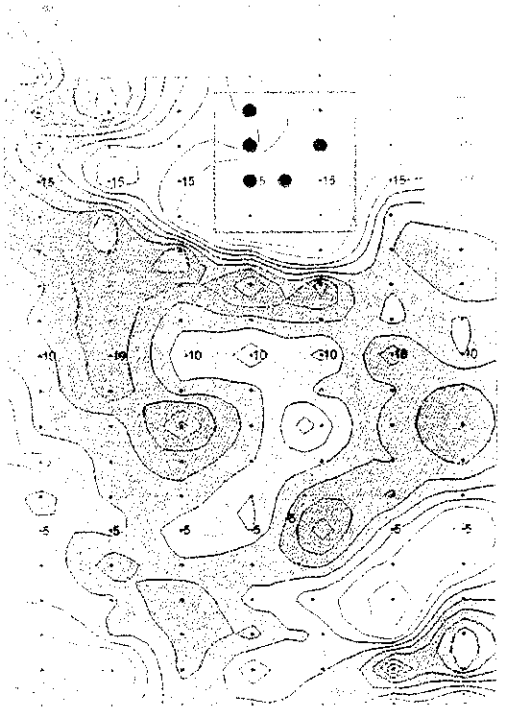
-15
-10
-5

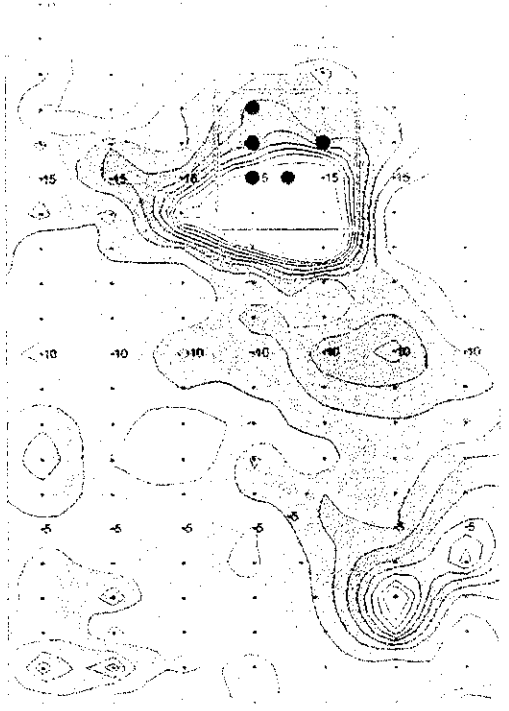
-15
-10
-5

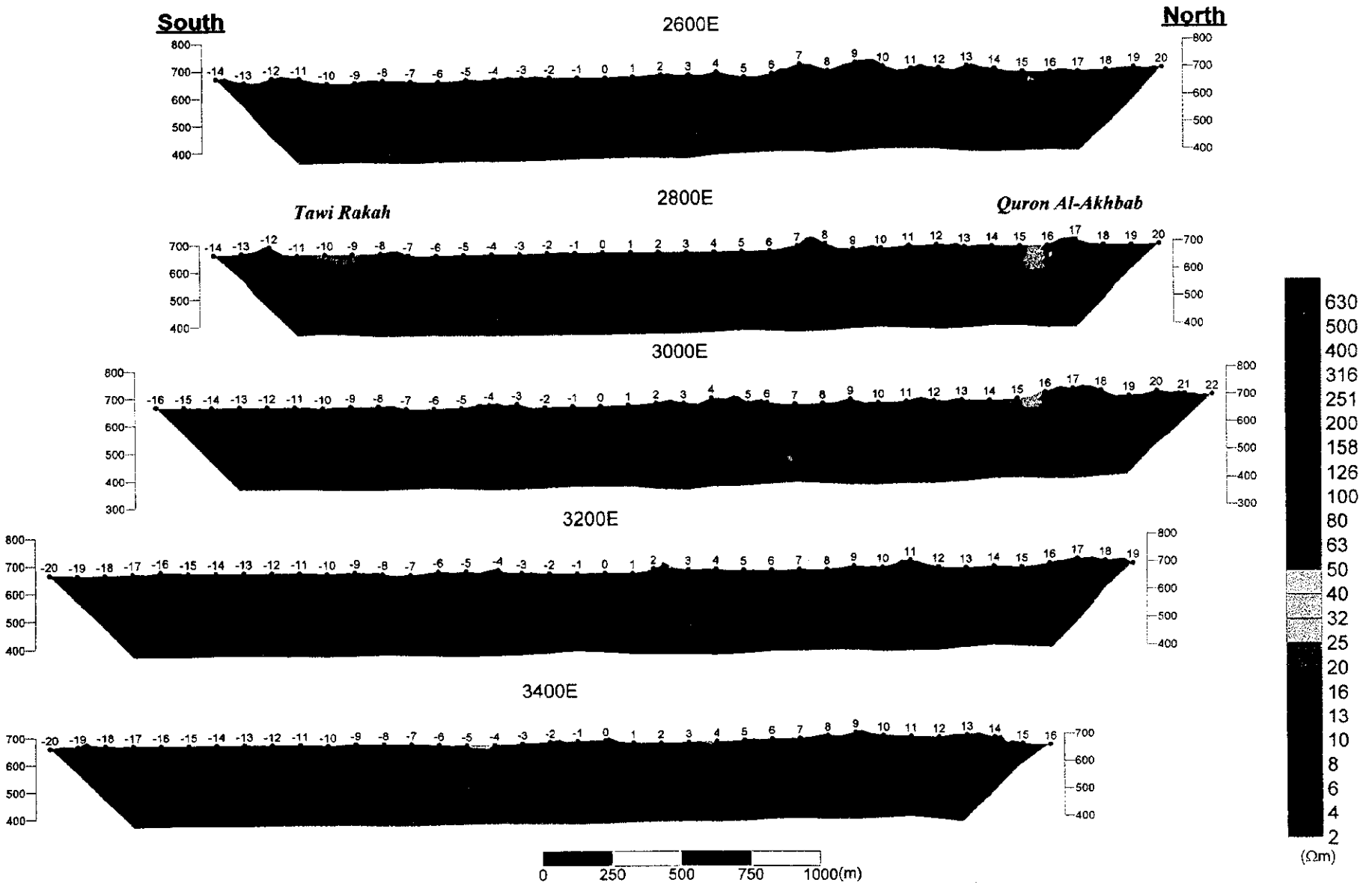

Fig. II-5-20(1) 2D analysis sections for resistivity in Quron Al-Akhbab and Tawi Rakah areas

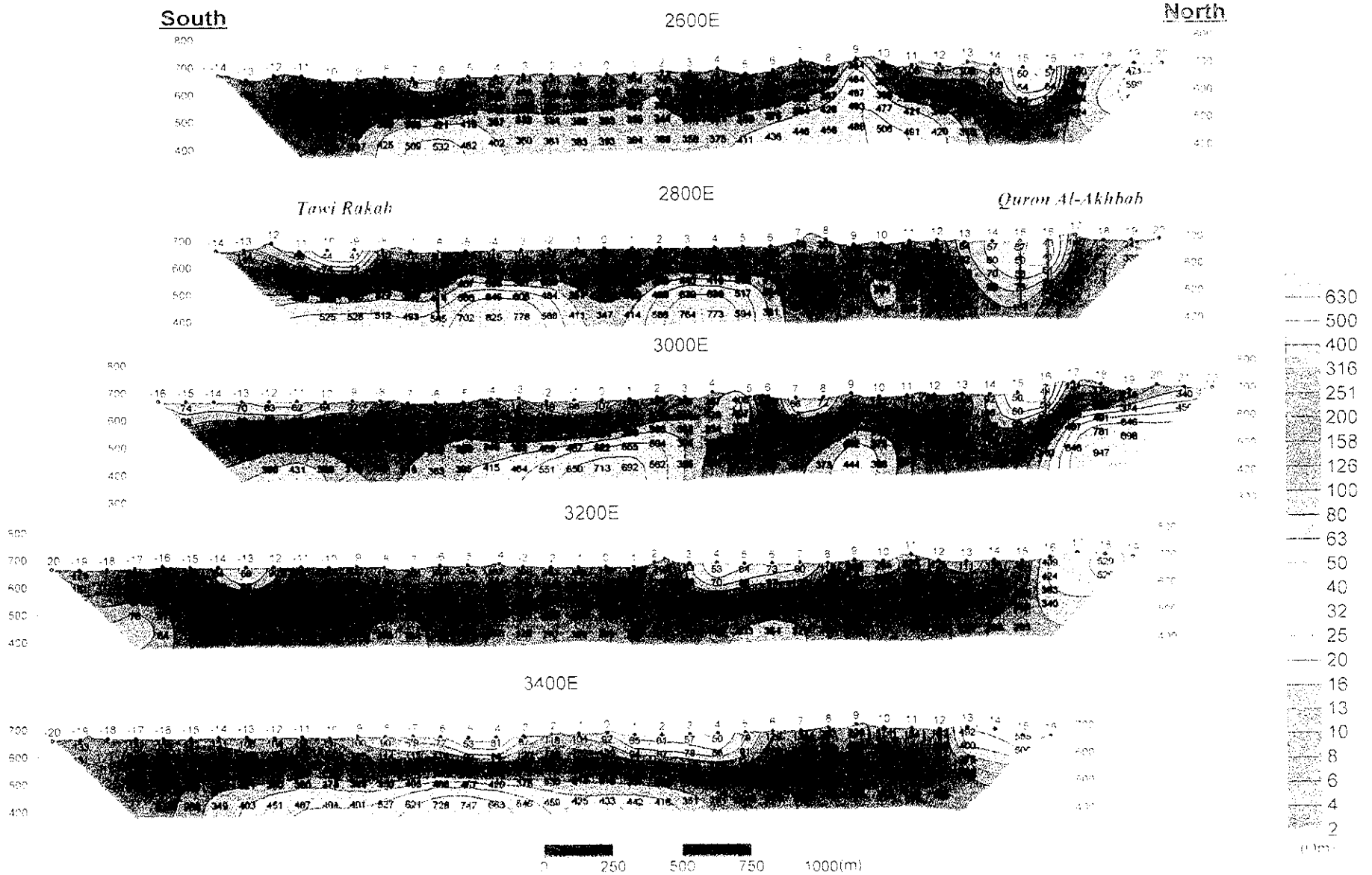

Fig. II-5-70(1) 2D analysis sections for resistivity in Quron Al-Akhbab and Tawi Rakah areas

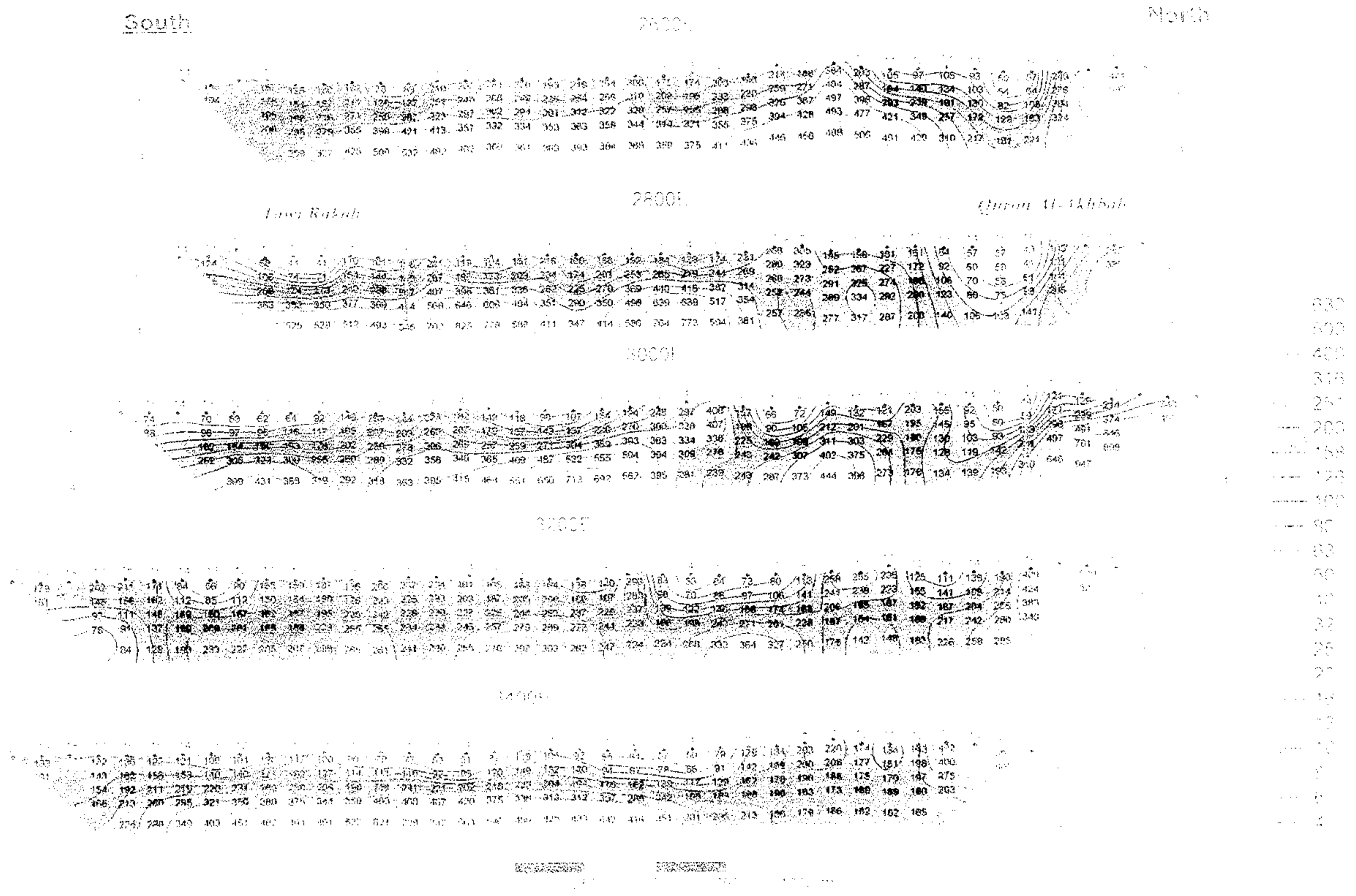
South
North
Lawi Rakah
Quron Al-Akhbah
2800E

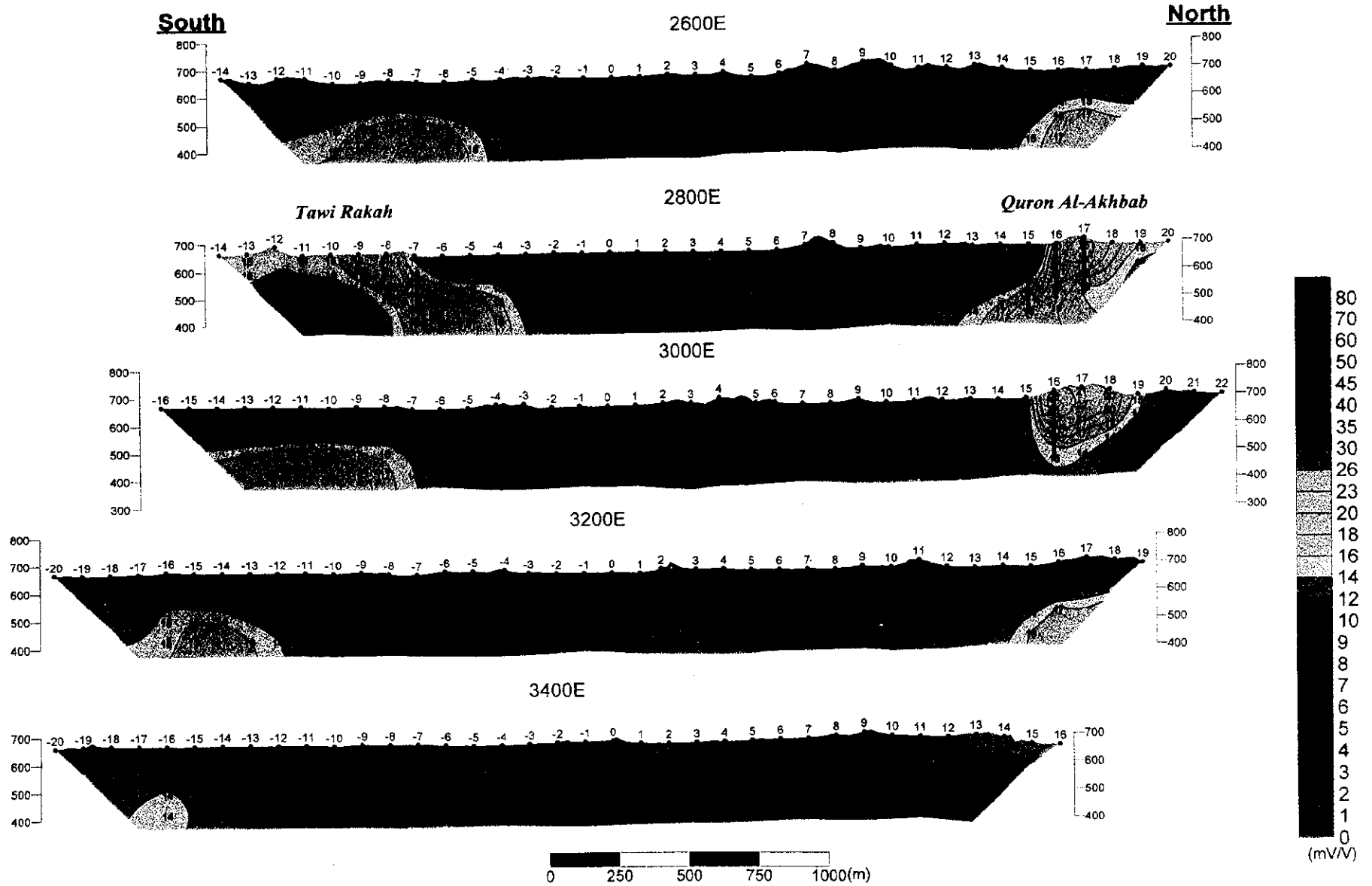

Fig. II -5-20(2) 2D analysis sections for Chargeability in Quron Al-Akhbab and Tawi Rakah areas

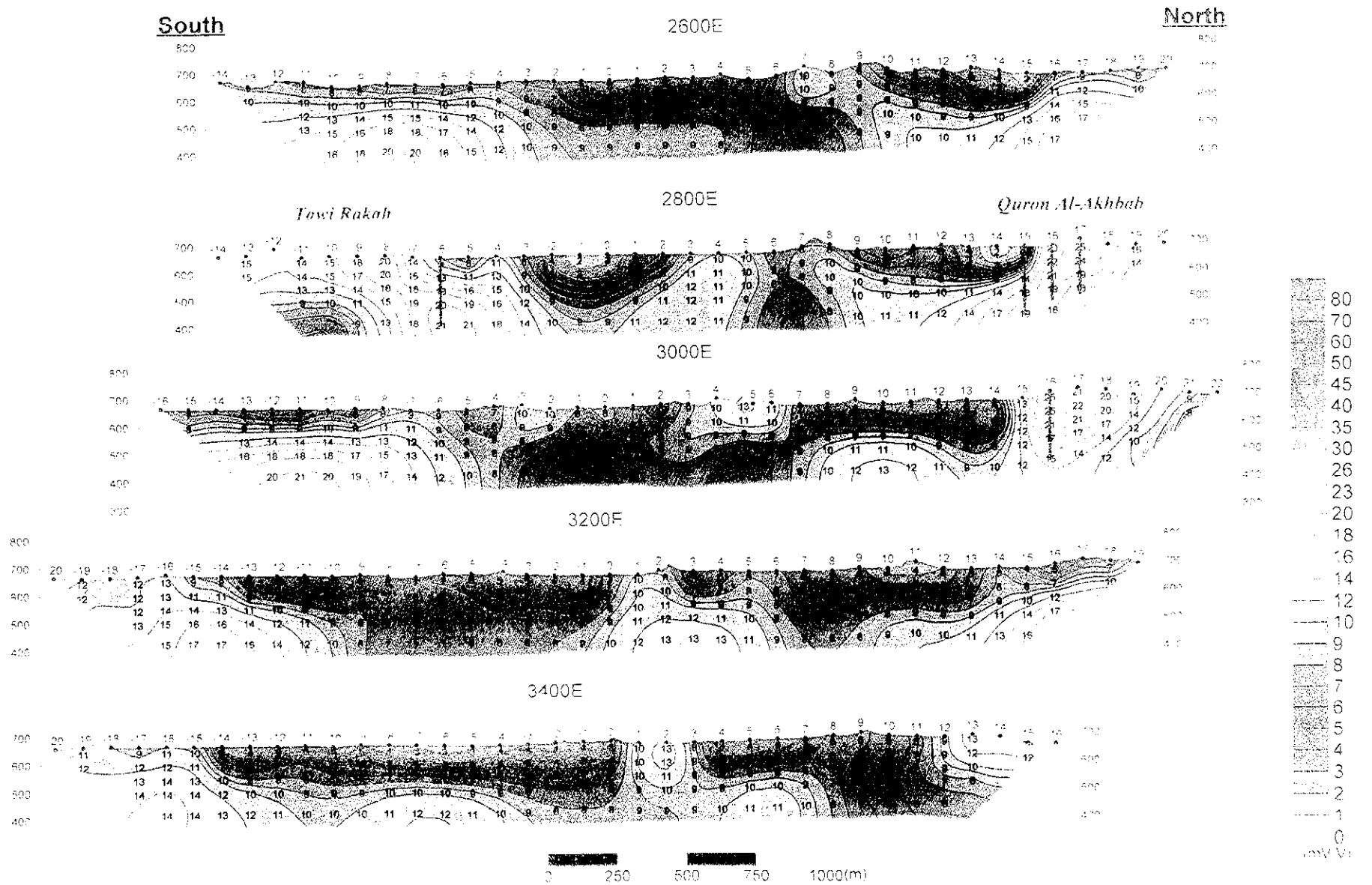

Fig. II-3-20(2) 2D analysis sections for Chargeability in Quron Al-Akhbab and Tawi Rakah areas

South

North

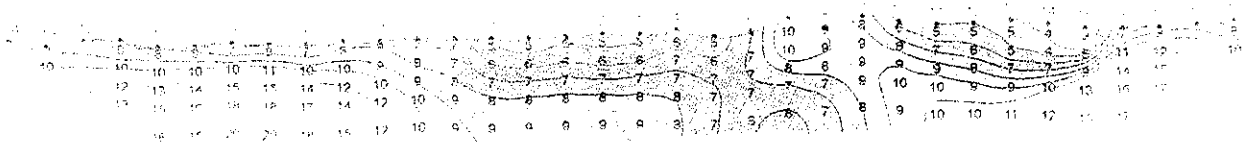

2800E

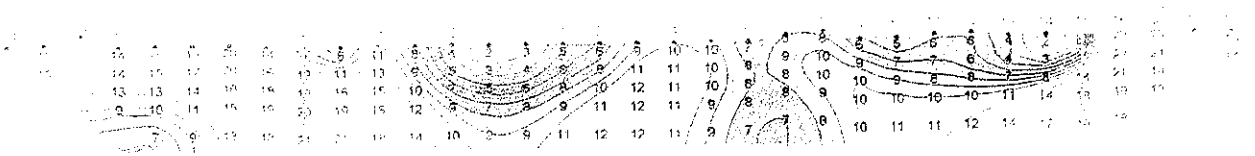

3000E

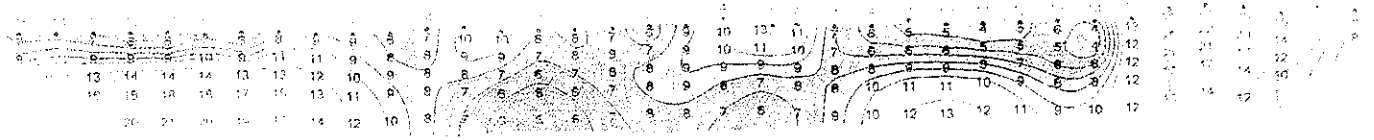

3200E

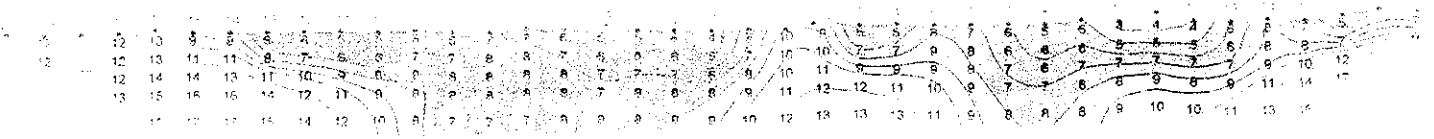

3400E

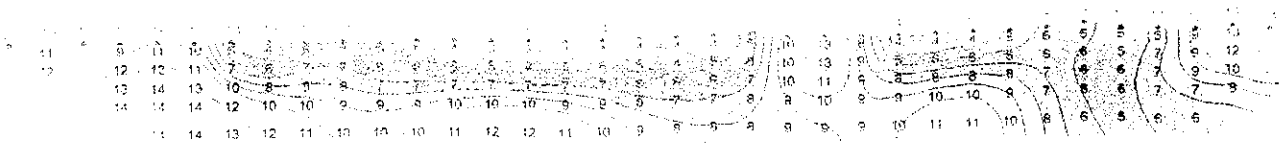

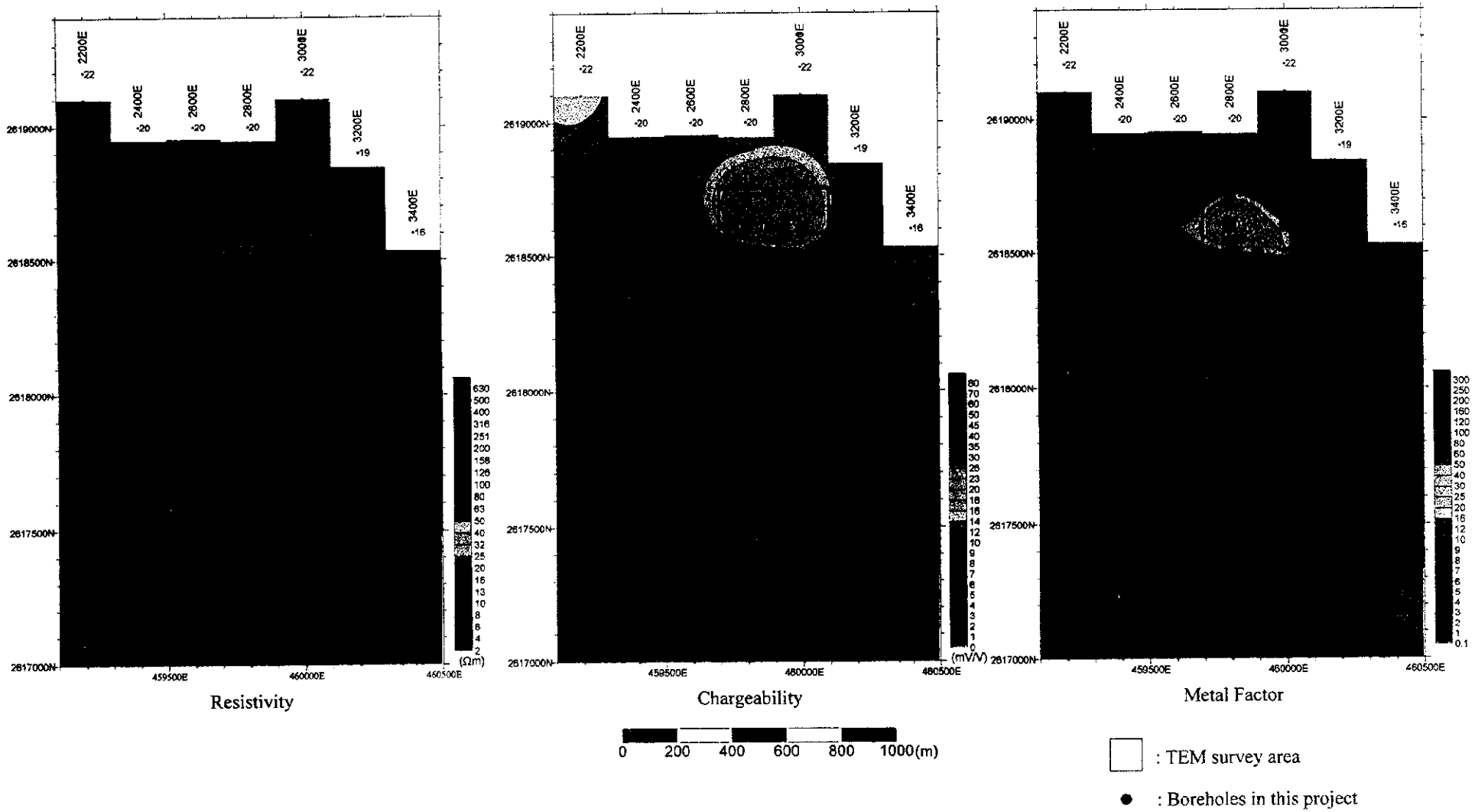

Fig. II -5-21(1) 2D analysis plane maps in Quron Al-Akhbab area at 100m depth

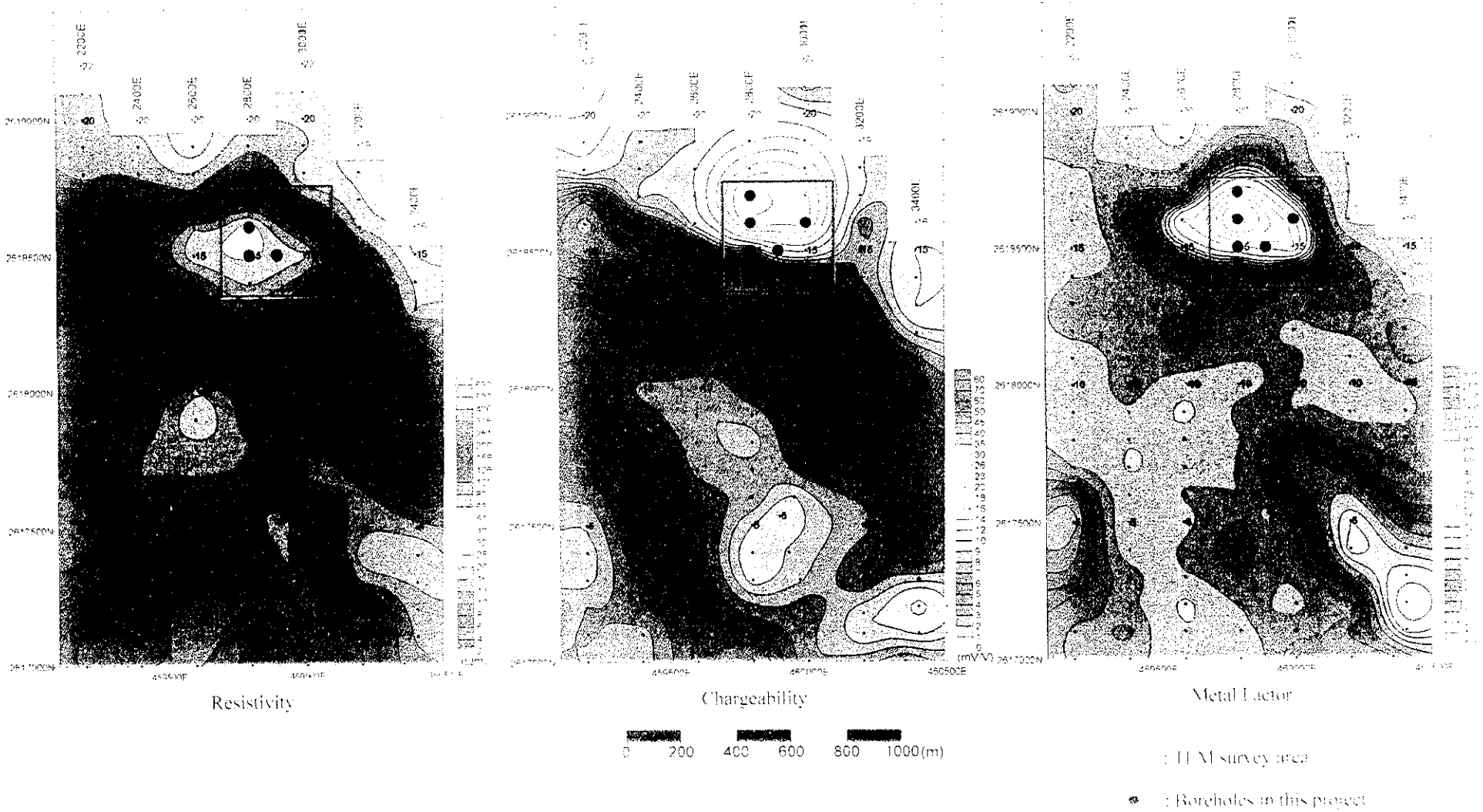

Fig. II-5-21(3) 2D analysis plane maps in Quron Al-Akhbab area at 100m depth

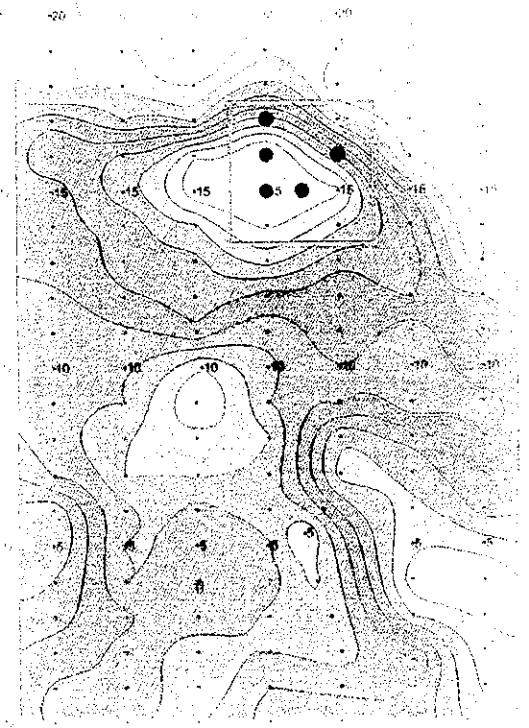

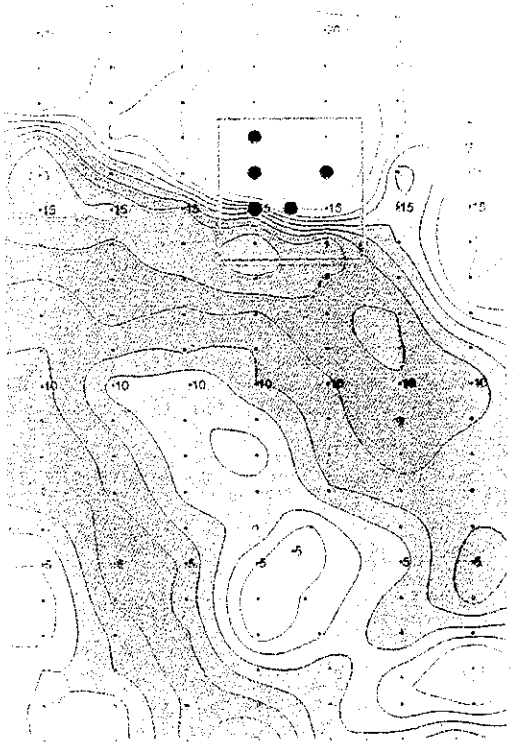

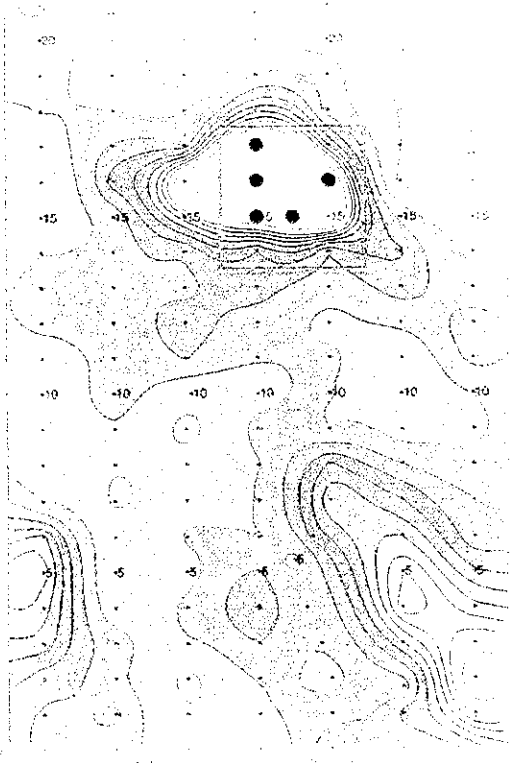

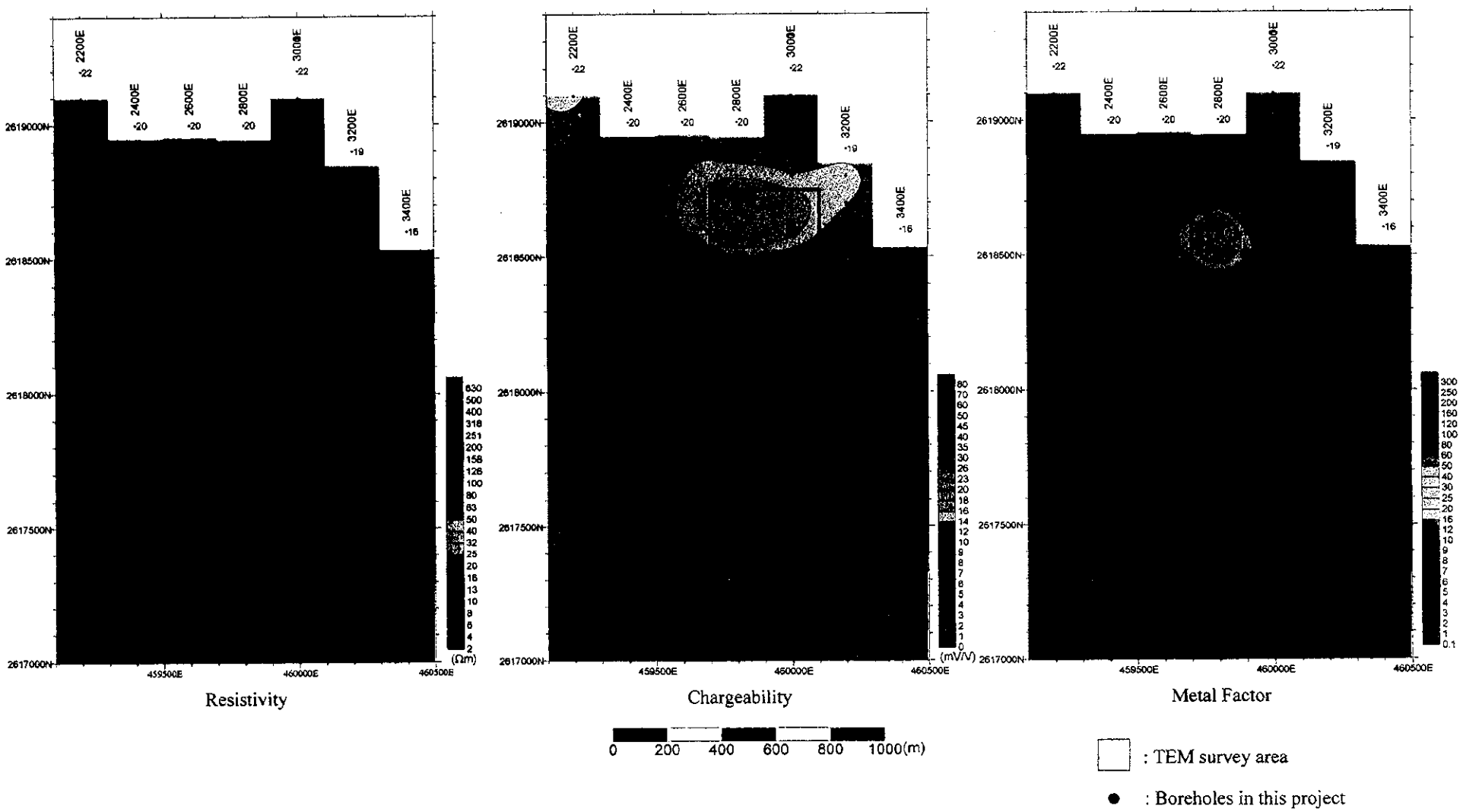

Fig. II -5-21(2) 2D analysis plane maps in Quron Al-Akhbab area at 150m depth

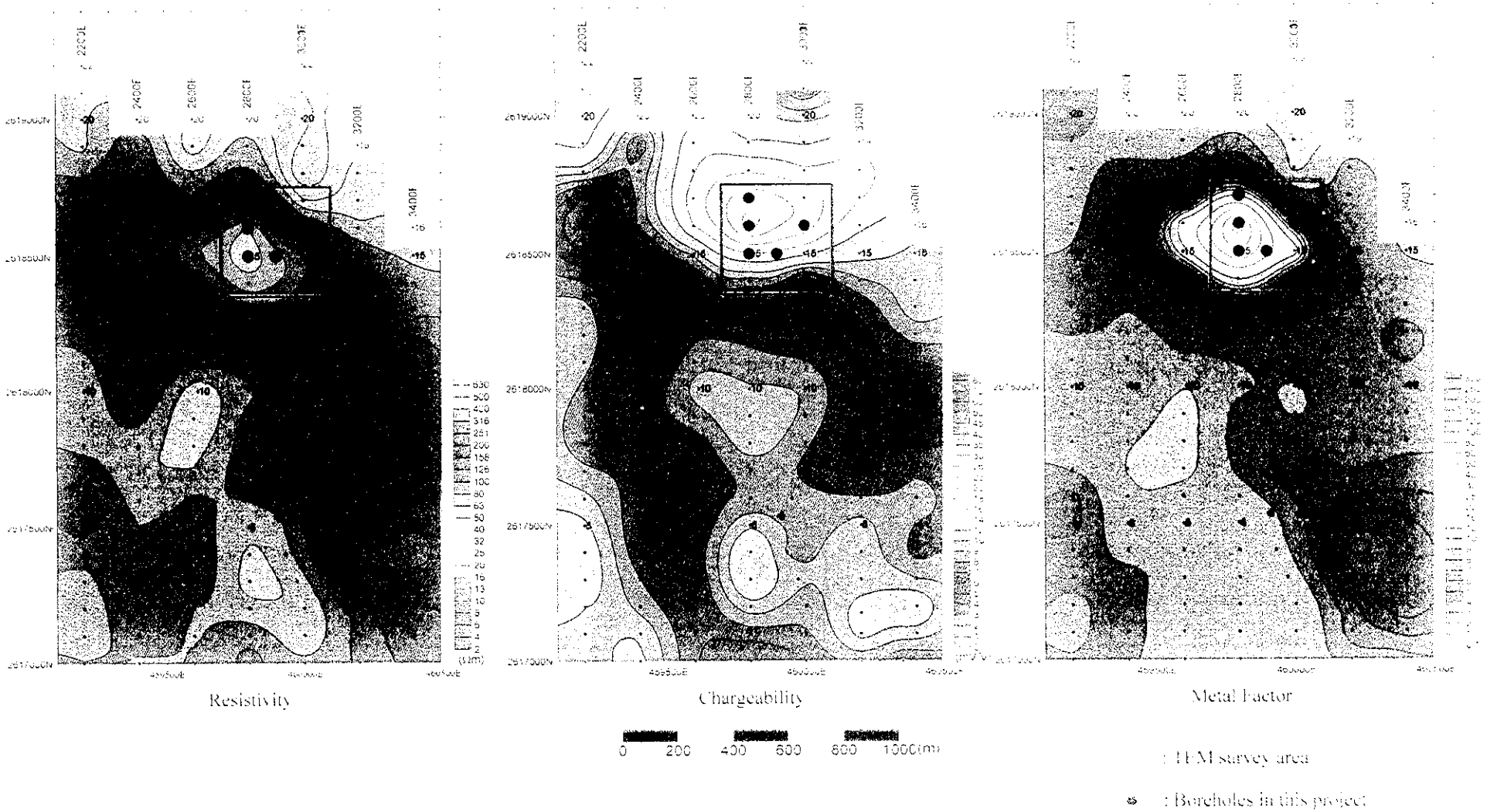

Fig. II-5-21(2) 2D analysis plane maps in Quron Al-Akhbab area at 150m depth


-20
-15
-10
-5

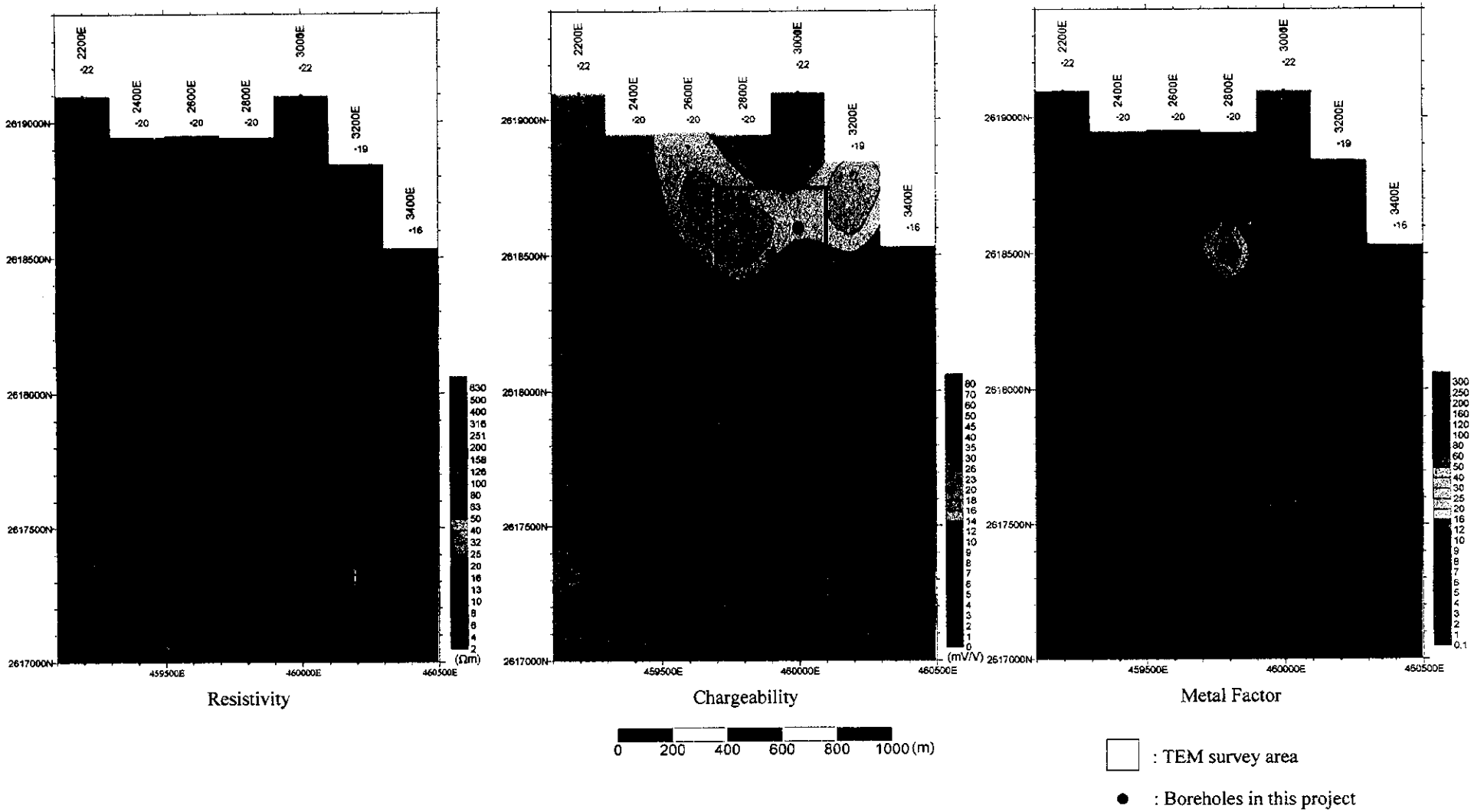

Fig. II -5-21(3) 2D analysis plane maps in Quron Al-Akhbab area at 200m depth

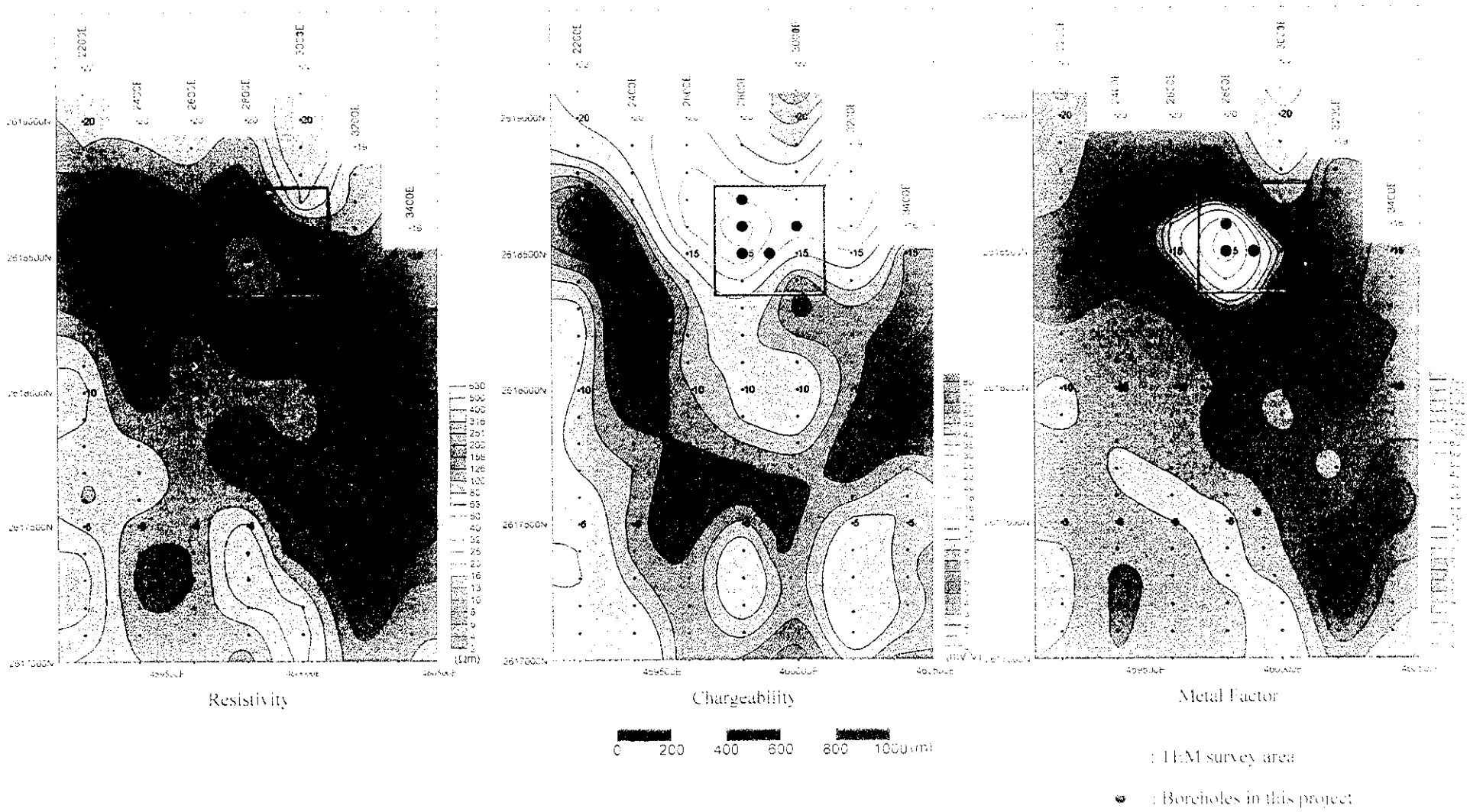

Fig. II-5-21(3) 2D analysis plane maps in Quron Al-Akhbab area at 200m depth

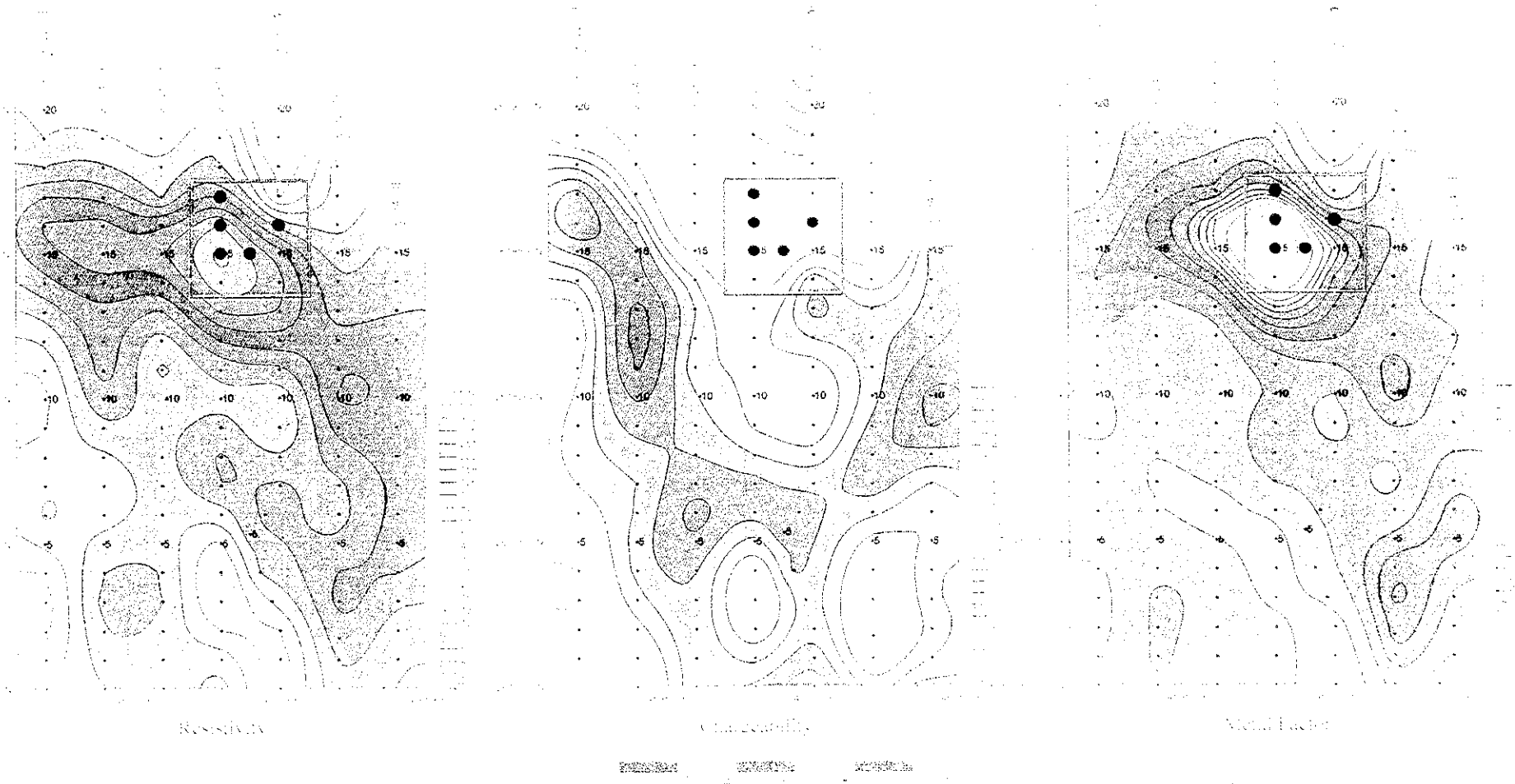
-20
-15
-10
-5
5
10
15

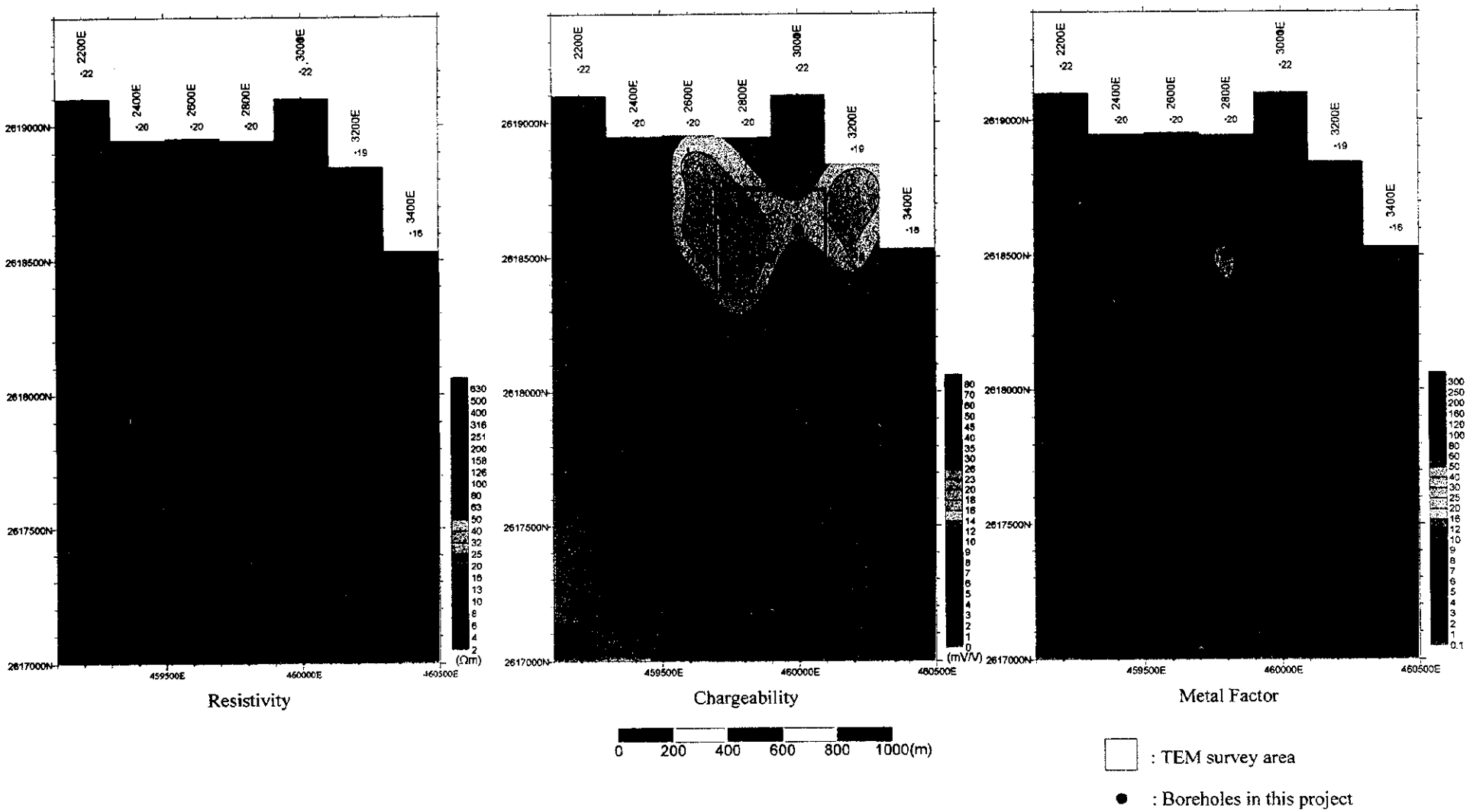

Fig. II -5-21(4) 2D analysis plane maps in Quron Al-Akhbab area at 250m depth

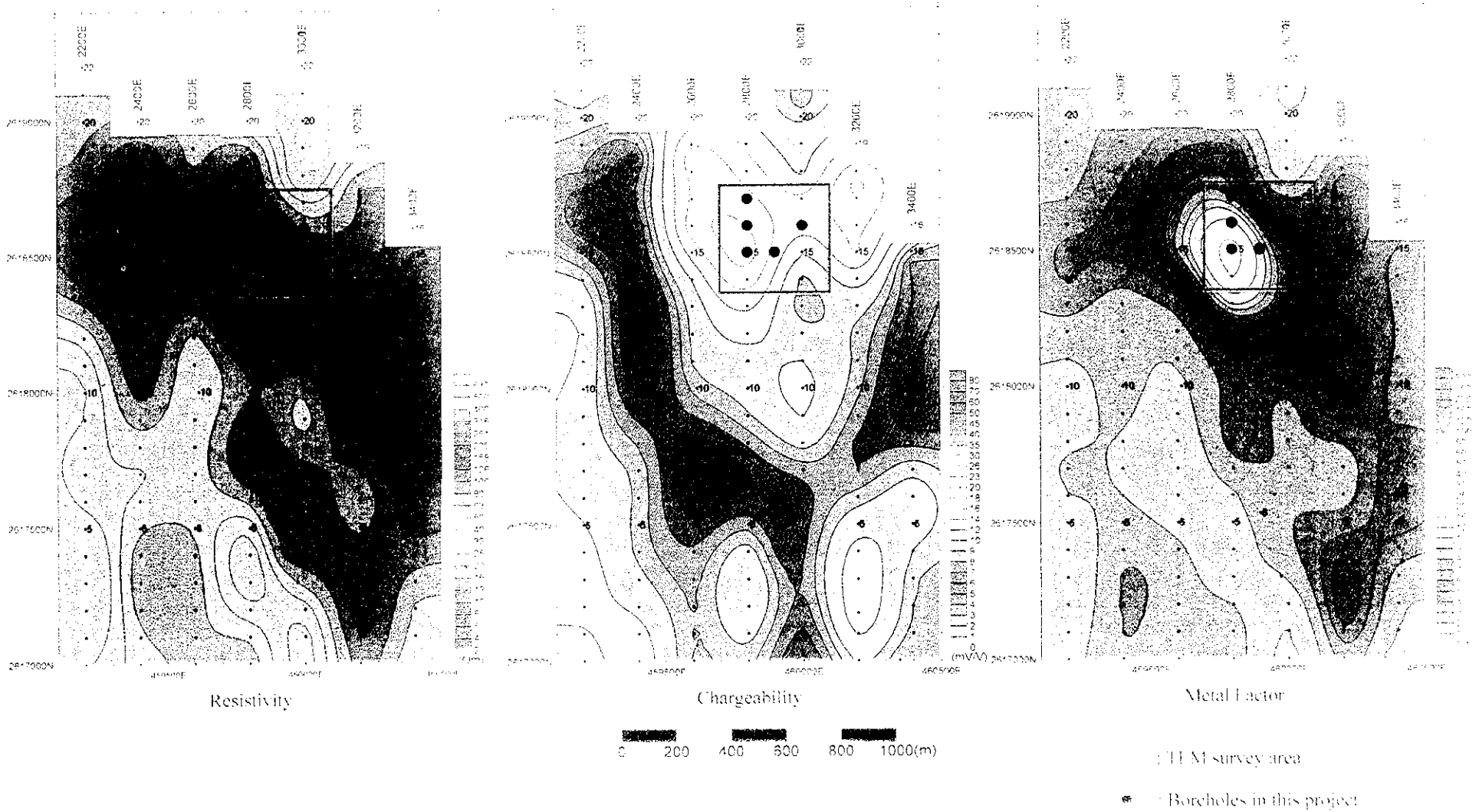

Fig. II-5-2(14) 2D analysis plane maps in Quron Al-Akhbab area at 250m depth

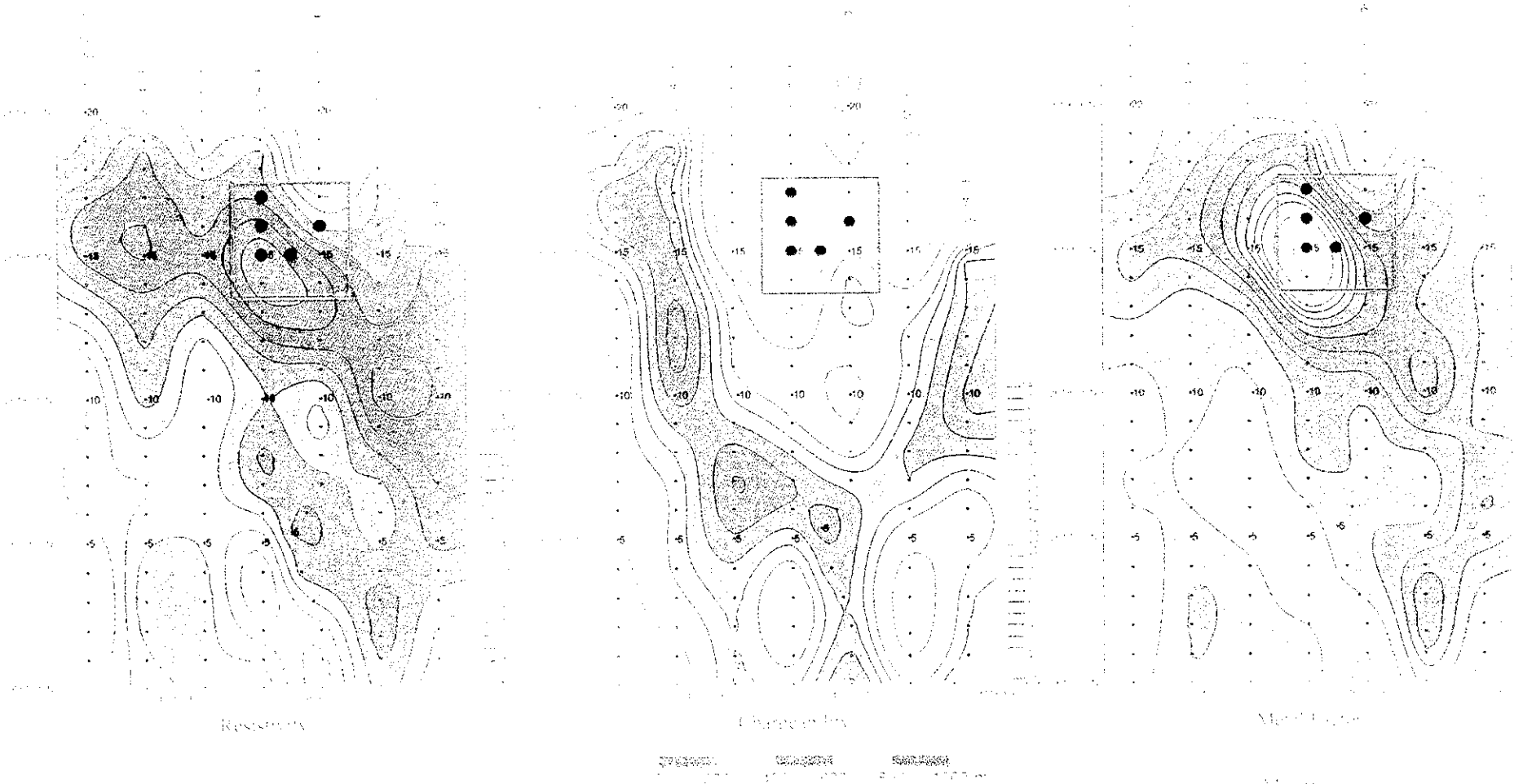

2800E. TEM was carried out around this portion to confirm the interesting detected IP values.

Drilling survey was carried out to confirm the interesting results of the TEM survey, but it failed to detect massive sulphide and instead, stockwork was intersected. When the results of TDIP, TEM and drilling are compared, no remarkable alteration was intersected in the place where resistivity was low, however, the place where high chargeability was detected and the place where stockwork was intersected agrees quite well. As a result, we can understand that stockwork shows high chargeability and medium to high resistivity. The low resistivity detected by the geophysical survey is probably not due to minelarization but mainly due to the effect of the underground water.

5-5-3 Tawi Rakah area

The TDIP results obtained in Tawi Rakah area are shown as plane maps in Figs. II-5-22 for N=1,4. 2D modeling are indicated as sections in the Figs. II-5-23 (Lines 2600E to 3400E) and as plane maps at the depth of 100m, 150m, 200m and 250m in Figs. II-5-24.

In the central part of the surroundings of the stations 900S and 1000S of line 2800E, it is confirmed low apparent resistivity and high chargeability. This anomaly seems to correspond to the Tawi Rakah mineral showings. Even though the low resistivity is limited at superficial levels, the high chargeability extends down to the levels N=2, 3 shifted to the south around the central part of the stations 1100S and 1000S.

High chargeability is confirmed in the northern part of line 2000E around the station 600S about 300m from Tawi Rakah showings at the depths indicated by the levels N=3,4. Due to the high resistivity values detected, TEM survey was not carried but one drilling was carried out on the center of the high chargeability anomaly.

Due to the results of the 2D analysis, low resistivity and high chargeability are limited only on the surface. The high chargeability distribution detected at deep part of the station 600 of the line 2800E is also seen in the result of 2D analysis, and extended to station 700S on the line 2600E. The high chargeability seen in the pseudosection at deep part of the stations 1000S to 1100S on the line 2800E is not seen in the results of the 2D analysis.

5-5-4 Hayl as Safil area

The results of the TDIP survey carried out in Hayl as Safil area and surroundings are indicated in Fig. II-5-24. The 2D results are indicated in Figs. II-5-25 and Fig. II-5-26. In this area, 4 ore bodies have been confirmed: Al Ashgar, Hayl as Safil, Bishara and Al Jadeed. Within Al Ashgar and Al Jadeed, a distribution of low chargeability and high chargeability is seen at N=1 which can lead to the discovery of massive sulphide. In Al Jadeed, low resistivity detected in the southern part appears as a response of low resistivity of the ore body and the sedimentary rocks of the southern part. The metal factor agrees well with the location of the ore body. At the depth of N=2, the anomaly disappears in both Al Ashagra and Al jaded, indicating that the continuity of the ore body cannot be expected at deeper parts.

In Bishara ore body, low resistivity and high chargeability are detected at N=1,2. The low